Orbital Interactions in Metal Dimer Complexes

P. Jeffrey Hay, Jack C. Thibeault, and Roald Hoffmann*

Contribution from the Department of Chemistry and Materials Science Center, Cornell University, Ithaca, New York 14853. *Received January 9, 1975*

Abstract: A molecular orbital analysis shows that the antiferromagnetic contributions to magnetic coupling, favoring a low-spin ground state for a dimer containing two weakly interacting metal centers, can be analyzed in terms of pairwise interactions of dimeric molecular orbitals, with the square of the splitting in energy between the members of a pair being a measure of the stabilization of the low-spin state. The effect of geometrical distortions, electronegativity, and variation of substituents on the magnetic interaction in dimeric systems is examined in detail for singly bridged $L_nM-X-ML_n$ (n = 3, 4, 5); $Cu_2Cl_6^{2-}$ and other doubly bridged species where the bridging ligands are halogens, OR, pyridine *N*-oxides, oxalate, squarate; and the acetate bridged dimers $Cu_2(RCOO)_4$. The emphasis is on d^9 Cu(II) dimers, but other transition metal systems are also analyzed.

Transition metal complexes containing more than one metal atom with unpaired electrons can generally be categorized according to their magnetic behavior into three main groups depending on the strength of the metal-metal interaction. In the *noninteracting* type the magnetic properties of the dimer (or polymer) are essentially unchanged from the paramagnetic monomer. In the *strongly interacting* type formation of relatively strong metal-metal bonds occurs, and the molecule will display simple diamagnetic behavior (for even numbers of electrons).

In this paper the properties of *weakly interacting* metal ions will be investigated. In such compounds this weak coupling between the electrons of the two metal ions leads to low-lying excited states of different spin which can be populated at thermal energies ($\leq$1000 cm^{-1}). The resulting magnetic behavior will be antiferromagnetic or ferromagnetic, depending on whether the low spin (spins paired) or high spin (spins parallel) state is the ground state, respectively. These interactions—often termed *superexchange* because of the large distances involved (3-5 Å) between the metal ions—have been observed in a wide variety of compounds.[1-5]

In experimental studies the magnetic interaction between spins $\mathbf{S}_A$ and $\mathbf{S}_B$ for atoms A and B is usually written in a form suggested originally by Heisenberg, Dirac, and Van Vleck[6]

$$H = -2J\mathbf{S}_A\cdot\mathbf{S}_B \quad (1)$$

where the coupling constant J is *positive* if the spins are parallel and *negative* if they are paired. (In this paper an unsubscripted J refers to the above expression, while a subscripted J_{ij} refers to a two-electron Coulomb integral.) If $|\mathbf{S}_A| = |\mathbf{S}_B| = S_A$ molecular states with total spin S = 0, 1, . . . , $2S_A$ are possible, and the energy difference between two states with spin S and $S - 1$ is given by

$$E(S) - E(S-1) = -2JS \quad (2)$$

In the most common case discussed here, $S_A = \frac{1}{2}$, and the triplet-singlet splitting, $E(1) - E(0)$, equals $-2J$.

The theoretical interpretation of superexchange interactions has traditionally been based on ideas developed for infinite solid lattices.[7,8] Since it has been realized empirically that the bridging atoms between the metal ions determine the sign and magnitude of the exchange interaction, these qualitative treatments focus on the various types of overlap interactions between the ligand atomic orbitals and the metal d orbitals. A number of quantitative implementations of a configuration interaction computational scheme have appeared.[9]

More recently there have been theoretical treatments[1,10,11] which seek to extend such analyses to the cases involving molecular, rather than atomic bridging species, with special interest in molecular dimers. Within this latter context this paper will attempt to provide a broader theoretical framework for the analysis of superexchange interactions. The scheme developed here seems capable of giving semiquantitative information about the effects on the ordering of spin states of geometrical distortions and of substituent changes for the general case of a molecular-bridged dimer.

Primarily we shall attempt to show that (a) the antiferromagnetic contributions to superexchange, which are usually the more important and more sensitive to changes in the system, can be analyzed in terms of pairwise interactions of dimeric MO's, ϕ_i and ϕ_j; (b) the square of the splitting in energy between these orbitals, $|\epsilon_i - \epsilon_j|^2$, may be used as a measure of stabilization of the low-spin molecular state; and (c) the energy and symmetry of the orbitals of the bridging group are crucial determinants of the level splitting pattern. The last point, to be illustrated by the analysis of several Cu(II) systems, will establish an obvious connection between antiferromagnetically coupled metal centers and the now well-established phenomenon of through-bond coupling of lone pairs or π electron systems in organic molecules.[12]

We begin by a discussion of the relationship between molecular orbital energies and magnetic exchange parameters.

Theory of the Electronic States of Weakly Interacting Metal Centers

In this section we shall discuss the electronic structure of two weakly interacting metal ions from two distinct, but equivalent, viewpoints: a molecular orbital description and a localized orbital description. After an analysis of the case of one unpaired electron on each metal atom (e.g., the d^9 case) the general d^n case will be treated.

Molecular Orbital Basis. In **1** we show a schematic inter-

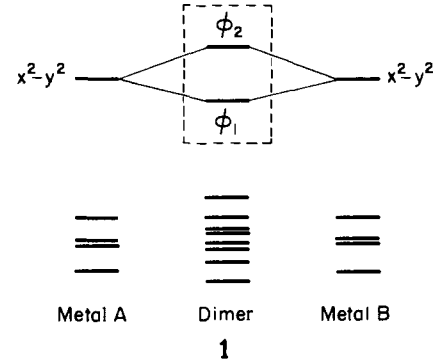

1

action diagram for the predominantly d-like orbitals of two weakly interacting square planar d^9 complexes, bridged by one or more atoms. In the absence of strong metal-metal bonding due to direct overlap of the d orbitals, the molecular orbital levels of the dimer will closely resemble the ligand field levels of the monomer, but the pairs of monomer levels will each be split slightly by the perturbation of the other metal atom.

For the d^9 case, where the unpaired electron occupies a $d_{x^2-y^2}$ orbital, we need focus only on the two highest levels formed from the two linear combinations of these (predominantly metal-like) orbitals, since the lower orbitals are all filled.

$$\phi_1 \sim d^a_{x^2-y^2} + d^b_{x^2-y^2}$$
$$\phi_2 \sim d^a_{x^2-y^2} - d^b_{x^2-y^2}$$

The following many-electron configurations arise from these orbitals:

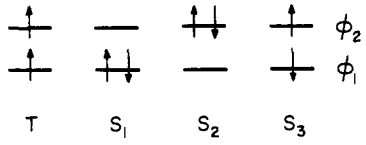

$$T: |\phi_1\alpha\ \phi_2\alpha|$$
$$S_1: |\phi_1\alpha\ \phi_1\beta|$$
$$S_2: |\phi_2\alpha\ \phi_2\beta|$$
$$S_3: 1/\sqrt{2}\,(|\phi_1\alpha\ \phi_2\beta| - |\phi_1\beta\ \phi_2\alpha|)$$

In this and succeeding discussions the MO's themselves are presumed to have been obtained from an SCF calculation on the *high-spin* (triplet) state.

The lowest singlet state of the system ψ_S will be an approximately equal mixture of S_1 and S_2

$$\psi_S = \lambda_1\psi_{S_1} + \lambda_2\psi_{S_2}$$

while the lowest triplet state is well represented by ψ_T. In the limit of noninteracting metal ions $|\lambda_1| = |\lambda_2|$, while in the opposite extreme $|\lambda_1| \gg |\lambda_2|$ for strong metal-metal bonding. (When ϕ_1 and ϕ_2 are of different symmetry, S_3 will be of different symmetry from S_1 and S_2, and in any case S_3 will correspond to an excited state much higher in energy.) The respective energies of the triplet and singlet states are as follows, after diagonalizing the 2×2 matrix involving S_1 and S_2.

$$E_T = h_1 + h_2 + J_{12} - K_{12} \tag{3}$$
$$E_S = h_1 + h_2 + \tfrac{1}{2}(J_{11} + J_{22}) - \tfrac{1}{2}[(2h_1 + J_{11} - 2h_2 - J_{22})^2 + 4K_{12}^2]^{1/2}$$

where

$$h_i = \int \phi_i^*(1)\hat{h}(1)\phi_i(1)\,d\tau_1$$
$$J_{ij} = \int \phi_i^*(1)\phi_j^*(2)\frac{1}{r_{12}}\phi_i(1)\phi_j(2)\,d\tau_1 d\tau_2$$
$$K_{ij} = \int \phi_i^*(1)\phi_j^*(2)\frac{1}{r_{12}}\phi_j(1)\phi_i(2)\,d\tau_1 d\tau_2$$

and $\hat{h}$ represents the core operator consisting of the kinetic energy, nuclear attraction, and all other electron-repulsion terms.

The quantity of interest, the singlet-triplet splitting, then becomes

$$E_T - E_S = -2J = J_{12} - K_{12} - \tfrac{1}{2}(J_{11} + J_{22}) + \tfrac{1}{2}[(2h_1 + J_{11} - 2h_2 - J_{22})^2 + 4K_{12}^2]^{1/2} \tag{4}$$

It will be useful to define orthogonal localized molecular orbitals (LMO's), ϕ_a and ϕ_b, as follows:

$$\phi_a = \frac{1}{\sqrt{2}}(\phi_1 + \phi_2) \tag{5}$$
$$\phi_b = \frac{1}{\sqrt{2}}(\phi_1 - \phi_2) \qquad \langle\phi_a|\phi_b\rangle = 0$$

ϕ_a will contain both metal and ligand character but will be essentially a d orbital on metal A, and ϕ_b will be the mirror image localized on metal B. In terms of these orbitals we have the following identities:

$$J_{11} = \tfrac{1}{2}(J_{aa} + J_{ab}) + K_{ab} + 2\langle aa|ab\rangle$$
$$J_{22} = \tfrac{1}{2}(J_{aa} + J_{ab}) + K_{ab} - 2\langle aa|ab\rangle$$
$$J_{12} = \tfrac{1}{2}(J_{aa} + J_{ab}) - K_{ab}$$
$$K_{12} = \tfrac{1}{2}(J_{aa} - J_{ab})$$

where the dominant terms are the one-center and two-center coulomb repulsion integrals J_{aa} and J_{ab}, respectively. When the splitting between h_1 and h_2 is small compared to K_{12} ($\approx \frac{1}{2}(10 - 5)$ eV = 2.5 eV), eq 4 becomes

$$E_T - E_S = J_{12} - \tfrac{1}{2}(J_{11} + J_{22}) + \frac{(h_1 - h_2)^2}{2K_{12}} \tag{6}$$

where we have neglected $J_{11} - J_{22}$ and terms of order $(1/K_{12})^2$. Finally we wish to make the correspondence between h_1 and h_2 and orbital energies ϵ_1 and ϵ_2. Since we have seen that neither S_1 nor S_2 is an adequate description of the singlet state, we consider the Hartree-Fock operator for the *triplet state* orbitals

$$\epsilon_1 = h_1 + J_{12} - K_{12}$$
$$\epsilon_2 = h_2 + J_{12} - K_{12}$$

and hence

$$h_1 - h_2 = \epsilon_1 - \epsilon_2$$

and

$$E_T - E_S = J_{12} - \tfrac{1}{2}(J_{11} + J_{22}) + \frac{(\epsilon_1 - \epsilon_2)^2}{2K_{12}}$$
$$= -2K_{ab} + \frac{(\epsilon_1 - \epsilon_2)^2}{J_{aa} - J_{ab}} \tag{7}$$

For the degenerate case $\epsilon_1 = \epsilon_2$, the triplet state is the ground state

$$E_S - E_T = 2J = 2K_{ab} \qquad (K_{ab} > 0)$$

while a significant splitting between the molecular orbitals ϕ_1 and ϕ_2 will yield a singlet ground state. Equation 7 suggests that we can focus on the difference of orbital energies, $\epsilon_1 - \epsilon_2$, as a measure of the singlet-triplet energy splitting. Such a relationship was also apparent from eq 3 without the simplifying assumptions leading to (7). It should also be noted here that expression 7 is not novel, with similar forms having been derived by others.[13,14] The superexchange problem in inorganic chemistry is very much akin to the diradical problem in organic chemistry where more than one configuration is needed for a proper description of a singlet ground state. Discussions similar to ours have been given concerning the singlet-triplet splitting and the state energies.[15]

The preceding MO analysis becomes unwieldy for the general case of more than one unpaired electron on each metal atom. For example, for a dimeric Ni^{2+} (d^8) complex with local octahedral symmetry about the metal ions the high-spin ($S = 2$) molecular state of the two weakly interacting $S = 1$ ions can be written (apart from the doubly occupied orbitals)

$$\psi(S = 2) = |\phi_1\alpha\ \phi_2\alpha\ \phi_3\alpha\ \phi_4\alpha|$$
$$\phi_1 \sim d^A_{x^2-y^2} + d^B_{x^2-y^2}$$
$$\phi_2 \sim d^A_{x^2-y^2} - d^B_{x^2-y^2}$$
$$\phi_3 \sim d^A_{z^2} + d^B_{z^2}$$
$$\phi_4 \sim d^A_{z^2} - d^B_{z^2}$$

The low spin ($S = 0$) state, however, will require major contributions from five configurations: $(\phi_1)^2(\phi_3)^1(\phi_4)^1$, $(\phi_2)^2(\phi_3)^1(\phi_4)^1$, $(\phi_1)^1(\phi_2)^1(\phi_3)^2$, $(\phi_1)^1(\phi_2)^1(\phi_4)^2$, and $(\phi_1)^1(\phi_2)^1(\phi_3)^1(\phi_4)^1$, and an analysis would have to deal with the 5×5 interaction matrix.

Localized Orbital Basis. In terms of the localized orbitals defined in eq 5, the d^9 case can be solved by perturbation theory in terms of the configurations

$$S'_4: 1/\sqrt{2}\,(|\phi_a\alpha\ \phi_b\beta| - |\phi_a\beta\ \phi_b\alpha|)$$

$$S'_{5a}: |\phi_a\alpha\ \phi_a\beta|$$

$$S'_{5b}: |\phi_b\alpha\ \phi_b\beta|$$

$$T': |\phi_a\alpha\ \phi_b\alpha|$$

where S'_4 is the "covalent" state and S'_{5a} and S'_{5b} are "ionic" states.

$$E_{S'_4} = h_a + h_b + J_{ab} + K_{ab}$$

$$E_{T'} = h_a + h_b + J_{ab} - K_{ab}$$

$$E_{S'_{5a}} = E_{S'_{5b}} = 2h_a + J_{aa} \quad (h_a = h_b)$$

Without admixture of the ionic states the singlet state will be very slightly above the triplet state

$$E_{T'} - E_{S'_4} = -2K_{ab} < 0$$

Configuration mixing will preferentially lower the singlet, since no ionic triplet states are possible

$$E_S \cong E_4 - \frac{\langle S_{5a}|H|S_4\rangle^2}{E_{5a} - E_4} - \frac{\langle S_{5b}|H|S_4\rangle^2}{E_{5b} - E_4}$$

$$= E_T + 2K_{ab} - \frac{(2h_{ab} + 2\langle aa|ab\rangle)^2}{J_{aa} - J_{ab} - K_{ab}}$$

$$E_T - E_S = -2K_{ab} + \frac{(2h_{ab})^2}{J_{aa} - J_{ab}} \tag{8}$$

where we have ignored the smaller two-electron integrals as before. This is the identical result obtained above in (3-4) using MO's since

$$2h_{ab} = \langle\phi_1 + \phi_2|h|\phi_1 - \phi_2\rangle = h_1 - h_2 = \epsilon_1 - \epsilon_2 \tag{9}$$

The preceding derivation is similar to Anderson's treatment of superexchange in insulators, which was based on an unrestricted Hartree-Fock formalism.[7] The ferromagnetic term $-2K_{ab}$ favoring the triplet corresponds to "potential exchange" in the Anderson model, and h_{ab} in the antiferromagnetic term favoring the singlet corresponds to the "transfer integral" in "kinetic exchange".

For the d^n case with m unpaired electrons on each metal atom one can usually group the MO's involving the unpaired electrons into m distinct pairs $[(\phi_1, \phi_2), (\phi_3, \phi_4), \ldots]$ of closely related orbitals from which localized orbitals can then be formed $[(\phi_{a1}, \phi_{b1}), (\phi_{a2}, \phi_{b2}), \ldots]$. A perturbation analysis of the energy differences of the spin states of the dimer ($S = 0, 1, \ldots, 2S_A$) for monomers with spin S_A yields the familiar result (eq 2)

$$E(S) - E(S-1) = -2SJ$$

consistent with the Heisenberg Hamiltonian, where J can be decomposed into orbital contributions. As in the above case with one unpaired electron, there will be ferromagnetic (J_F) and antiferromagnetic (J_{AF}) contributions

$$J_F = \frac{1}{m^2}\sum_{i\in A}\sum_{j\in B} K_{ij}$$

$$J_{AF} = -\frac{1}{m^2}\sum_{i=1}^{m}\frac{\frac{1}{2}(\epsilon_{2i} - \epsilon_{2i-1})^2}{J_{ai,ai} - J_{ai,bi}}$$

where the second sum is over the distinct pairs of MO's.

The specific example of two high spin d^8 monomers is worked out in detail in Appendix 1. The result

$$2J = -E(S=1) + E(S=0) = \tfrac{1}{2}[-E(S=2) + E(S=1)] = \tfrac{1}{2}(K_{ac} + K_{ad} + K_{bc} + K_{bd}) - \frac{\frac{1}{4}(\epsilon_1 - \epsilon_2)^2}{J_{aa} - J_{ac}} - \frac{\frac{1}{4}(\epsilon_3 - \epsilon_4)^2}{J_{bb} - J_{bd}}$$

where ϕ_1 and ϕ_2 are the MO's involving the $x^2 - y^2$ orbitals ($\phi_a{}^A$ and $\phi_c{}^B$) and ϕ_3 and ϕ_4 involve the z^2 orbitals ($\phi_b{}^A$ and $\phi_d{}^B$), shows that the antiferromagnetic terms can be traced to the *separate* contributions of the $(x^2 - y^2)$-like and z^2-like orbitals, respectively.

Nonorthogonal Orbital Basis. In the two preceding frameworks the inclusion of configuration interaction was needed: in the former case by mixing the doubly excited state $\phi_2{}^2$ with $\phi_1{}^2$, and in the latter case by including ionic states. It is possible to retain a one-electron single-configuration representation by using nonorthogonal orbitals. The singlet wave function in terms of LMO's

$$|(a\bar{b} - \bar{a}b)|/\sqrt{2} + \lambda(|a\bar{a}| + |b\bar{b}|)$$

can be rewritten as

$$|a'\bar{b}' - \bar{a}'b'|/\sqrt{2}$$

if one defines

$$\phi_a' = \phi_a + \frac{\lambda}{\sqrt{2}}\phi_b$$

$$\phi_b' = \phi_b + \frac{\lambda}{\sqrt{2}}\phi_a$$

$$\langle\phi_a'|\phi_b'\rangle \neq 0$$

If ϕ_a' and ϕ_b' are chosen to be atomic orbitals, the wave function corresponds to the Heitler-London type. ϕ_a' and ϕ_b' can be optimized self-consistently as in the GVB[16] and spin-projected unrestricted Hartree-Fock methods,[17] which can be extended to n electrons per metal ion. They would also correspond approximately to the "oligomer MO's" of Dance.[11]

Superexchange and the Extended Hückel Framework. The preceding analysis, if perhaps somewhat belabored, has attempted to establish the link between antiferromagnetic exchange interactions and the difference in energies between otherwise degenerate MO's. The orbital energies in this paper are obtained from extended Hückel calculations[18]—the simplest all valence-electron model. Details of the procedures we used are given in Appendix 2. Although these calculations do not explicitly include two-electron interactions, the behavior of the levels is expected to reflect what one would observe in more sophisticated calculations. To the extent that the qualitative changes in these orbital energies as a function of structure and substituents are reproduced by extended Hückel theory, one would expect this simple one-electron model to treat the AF part of the exchange interaction. Since two-electron interactions are not explicitly included in the theory, actual singlet-triplet energy differences cannot be computed. In the two-electron case, where

$$E_T - E_S = -2K_{ab} + \frac{2(\epsilon_1 - \epsilon_2)^2}{J_{aa} - J_{ab}}$$

we would focus on the quantity $(\epsilon_1 - \epsilon_2)$ since the denominator should be a fairly slowly varying quantity as a function of distortions or substituent effects for closely related compounds. The same considerations should apply to K_{ab}, which is usually small ($\sim$1-50 cm^{-1} experimentally) and dominated by the second term.

The reader should note the terminological bind we are in.

The study of magnetic interactions in metal complexes is traditionally tied to a spin Hamiltonian, with experimental results uniformly expressed in terms of the above mentioned coupling constant J. Words such as "ferromagnetic" and "superexchange", when taken literally, relate to the spin formalism. On the other hand we have shown a relationship between the singlet-triplet gap and the splitting of pairs of one-electron energy levels. We will examine the effect of geometry and substituents on the low-spin high-spin energy difference through the perturbations of these levels. Our problem is in comparing our theoretical inferences, expressed in terms of diminished or increased energy gaps, with experimental results phrased in the spin formalism, expressed in terms of "superexchange", "significant antiferromagnetic (AF) coupling", or "large negative J". We will often opt for any of these terms, but our meaning should be clear.

Influence of Bridging Angle on Spin State

The effect of the metal-ligand-metal bridge angle on the exchange interaction has been studied extensively, and a qualitative justification has been provided by the Goodenough-Kanamori rules[8] and the Anderson model.[7] Such considerations lead one to expect a large AF coupling for a 180° bond angle when the metal orbitals can interact with a ligand orbital of the same symmetry, and a weak F coupling for a 90° bond angle when the metal orbitals are interacting through orthogonal ligand orbitals.

Although our analysis will yield the same qualitative predictions as to the effect of bond angles, we shall use these results to show the consistency of the MO approach with previous interpretations and to justify its application later to more complex systems.

A comprehensive discussion of the structural and magnetic evidence for the angular dependence of metal-metal interactions of Cu(II) and Cr(III) systems has been presented by Hodgson.[19] He provides a perceptive theoretical discussion which has many parallels to our qualitative analysis.

Dimers with Single Bridging Atoms. Consider first the hypothetical case of $Cu_2Cl_7^{3-}$, two square planar $CuCl_4^{2-}$ complexes joined by a single atom. In the d^9 monomer the unpaired electron occupies an $x^2 - y^2$ orbital oriented along the bond axes.[20] (Throughout this paper we will use the abbreviated notation for p and d orbitals, $x^2 - y^2$ standing for $d_{x^2-y^2}$, z for p_z, etc.) The highest occupied orbitals of the dimer are the symmetric (ϕ_S) and antisymmetric (ϕ_A) combinations of the monomer $x^2 - y^2$ orbitals, shown in **2**. We proceed to bend the dimer in such a way that each

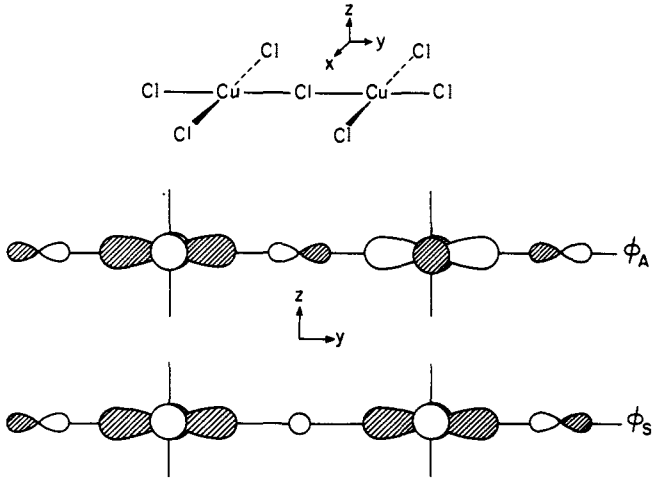

2

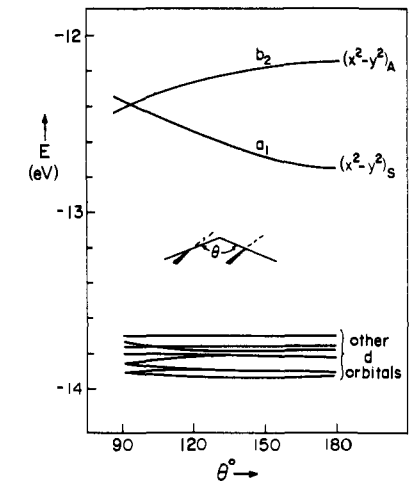

Figure 1. Energies of metal orbitals of $Cu_2Cl_7^{3-}$ as a function of bending at the bridging chlorine.

$CuCl_4$ fragment is kept planar as the Cu atoms move in a plane perpendicular to the original molecular plane. The orbital energies as a function of Cu-Cl-Cu angle θ are shown in Figure 1. For $\theta = 180°$ ϕ_A is higher in energy than ϕ_S, and as θ decreases the energy difference becomes smaller until at $\theta = 90°$ the two are practically degenerate. According to our previous discussion the factor $(\epsilon_S - \epsilon_A)^2$ favoring a singlet state would have its maximum value at $\theta = 180°$, while a triplet ground state would be expected near 90° when $\epsilon_S = \epsilon_A$.

This behavior may be understood from the interactions of the d orbitals with the lower-lying filled orbitals of the bridging atom. The local square planar environment about each metal orients the highest molecular orbital into a local "$x^2 - y^2$" orbital pointing along the M-L bonds. For the linear case, the symmetric combination (ϕ_S) of d orbitals can interact with the 3s orbital of the bridging Cl, and the antisymmetric combination (ϕ_A) can interact with the $3p_x$ orbital. This was shown in **2**. Since the metal 3d (−14.0 eV) is much closer in energy to the Cl 3p (−15.6) than the 3s (−27.1), the d-p interaction is much stronger and ϕ_A is shifted upward more than ϕ_S.

As the molecule is bent, the overlap of the $d_a - d_b$ combination with p_x decreases, since the d orbitals' local field constrains them to point approximately along the bond directions. This is shown in **3**. The antibonding character in

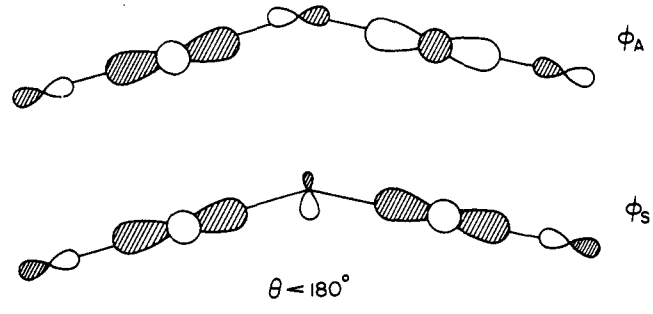

3

ϕ_A is reduced, and the orbital energy consequently decreases with bending. Although the $d_a + d_b$ interaction with the 3s orbital is unaffected, in bent geometries it begins to interact with the much higher-lying $3p_z$ Cl orbital—leading to an *increase* in antibonding character and a *rise* in energy. At 90° the d-p_x and d-p_z overlaps are identical, and one would thus expect comparable orbital energies, apart from the small d-3s interactions.

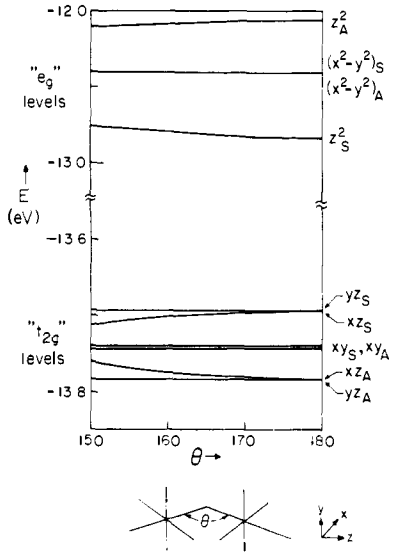

Figure 2. Orbital energies of Cu_2Cl_{11} as a function of bending at the bridging chlorine. Note the broken energy scale; the top of the figure is also on a different scale than the bottom.

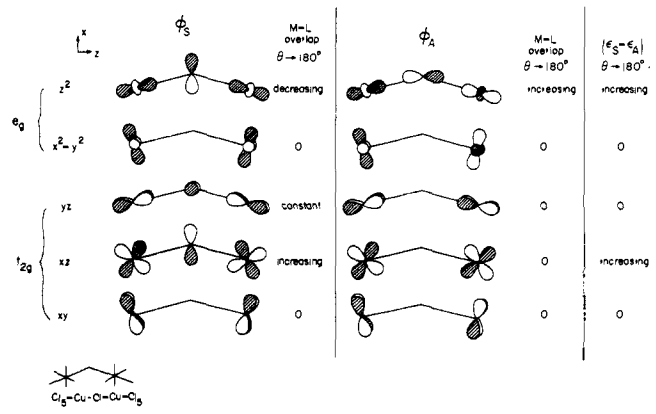

Figure 3. Schematic analysis of the various orbital trends as Cu_2Cl_{11} bends. Next to each orbital drawing is an indication of how the absolute value of the metal-ligand overlap in that orbital varies with bending. At right is a summary of the net effect on $|\epsilon_S - \epsilon_A|$.

Examples of monobridged dimers include the d^3 system Cr(III)-O-Cr(III)[21a-c] in $[(NH_3)_5Cr\text{-}O\text{-}Cr(NH_3)_5]^{4+}$ and the d^5 system Fe(III)-O-Fe(III)[5,21e] in $[((HEDTA)\text{-}Fe)_2O]^{2-}$. In these systems each metal ion has a pseudo-octahedral environment as contrasted with our previous square planar hypothetical example. To provide a qualitative guide to the superexchange processes in these d^n systems, the energy levels and orbitals of a model $[Cl_5Cu\text{-}ClCuCl_5]^{7-}$ dimer as a function of bridging angle ($150° \leq \theta \leq 180°$) are shown in Figures 2 and 3. Smaller angles were not considered because of steric repulsion between the terminal Cl ions. Although Cu is a d^9 system, the shapes of the orbitals and the trends of the energy levels will be unaffected by the differences in orbital occupancies. We must note at this point the classical molecular orbital analysis for oxo-bridged species of Dunitz and Orgel[22] and the more recent studies of Jezowska-Trzebiatowska and collaborators[23] and of Glerup.[24]

For the linear D_{4h} geometry one can easily analyze the various contributions to superexchange in terms of (ϕ_S, ϕ_A) pairs since each linear combination of the d-like orbitals has a distinct symmetry. The largest contribution comes from the (z^2_A, z^2_S) pair with an $\epsilon_A - \epsilon_S$ difference of 0.77 eV. As in the square-planar monomer case, the splitting—with ϕ_A higher in energy than ϕ_S—arises from the strong antibonding interaction of the $z^2_a - z^2_b$ combination with the filled z ligand orbital compared with the much weaker antibonding nature of the $(z^2_a + z^2_b)$-3s interaction. The following order is obtained for the five possible antiferromagnetic contributions in terms of the magnitude of the $\epsilon_A - \epsilon_S$ splitting: z^2 (0.77 eV) $\gg$ xz (0.09 eV) = yz (0.09 eV) > $x^2 - y^2$ (0 eV) = xy (0 eV). The splitting in the xz, yz pair arises from the antibonding $xz_s - x$ interaction in ϕ_S compared with no M-L interaction in ϕ_A, and the smaller magnitude reflects the weaker nature of $d\pi$-$p\pi$ overlap. Of course, when both S and A orbitals are filled or are empty, no stabilization occurs, so that AF coupling in d^3 dimers arises only from the t_{2g} members (xz, yz, xy), in d^8 dimers, from the e_g (z^2, $x^2 - y^2$), and in d^5 dimers, from all five.

For bent C_{2v} geometries the situation is at first sign less clear, since several MO's will now have the same symmetry. One can still decompose the interaction into the five components since the local octahedral environment serves to orient the d orbitals of the dimer. For example, the $z^2_a + z^2_b$, $(x^2 - y^2)_a + (x^2 - y^2)_b$, and $xy_a - xy_b$ combinations in terms of space-fixed coordinates recombine to give (a) an $x^2 - y^2$ MO in terms of the local coordinates of the metal with a very small ligand component on the bridging atom, (b) a z^2-like orbital oriented along the L_b-M-L_a bond with ligand 2s character, and (c) an xy-like orbital (see Figure 3). The slopes of the orbitals in Figure 2 can all be understood in terms of the changes in antibonding character as a function of θ. By way of an example let us look at the xz and yz orbitals. The xz_S MO loses antibonding character on bending, while xz_A has no ligand mixing. Consequently $|\epsilon_S(xz) - \epsilon_A(xz)|$ decreases with bending, and with it decreases the contribution of this MO to metal-metal interaction. In contrast the yz orbital splitting does not change with bending, for the yz_S-bridging ligand orbital interaction is unaffected by the distortion.

The reduction in xz orbital splitting with bending is one reason why in the case of the Cr(III) dimer the oxo-bridged form ($\theta = 180°$)[21a-c] shows a much larger antiferromagnetic interaction ($2J = -450$ cm^{-1}) than the hydroxo-bridged form ($\theta = 166°$, $2J = -32$ cm^{-1}).[21a-d] A referee has correctly noted that the difference in interaction could be a consequence of the significantly different Cr-O bond distances in the two families. In the Fe(III) series, a direct comparison of two known species with different bridge angles is less straightforward, since the compound with large angle ($\theta = 165°$), $[(HEDTA)Fe)_2O]^{2-}$, contains an oxo bridge ($2J = -85$ cm^{-1}) while one compound with small angle, $[Fe(pic)_2OH]_2$, contains two OH bridges ($2J = -8$ cm^{-1}).[25] A case where the z^2 splitting is sufficiently large to cause a diamagnetic d^7 dimer with $(z^2_S)^2$ occupancy apparently occurs in the Co(II)-I^--Co(II) dimer which is diamagnetic and contains a linear Co-I-Co bridge.[26]

Doubly Bridged Dimers. Recent experimental work[27] has provided a more extensive probe of metal-metal interaction as a function of Cu-L-Cu bond angle in the case of the di-bridged species **4** where L = OH^-. We have studied the

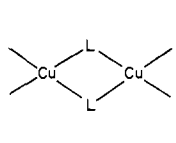

4

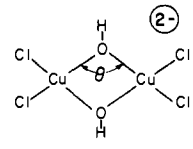

5

model planar system **5**. All bond lengths ($R_{Cu\text{-}Cl}$ = 2.26 Å, $R_{Cu\text{-}O}$ = 1.92 Å, $R_{O\text{-}H}$ = 0.95 Å) and the Cl-Cu-Cl angle

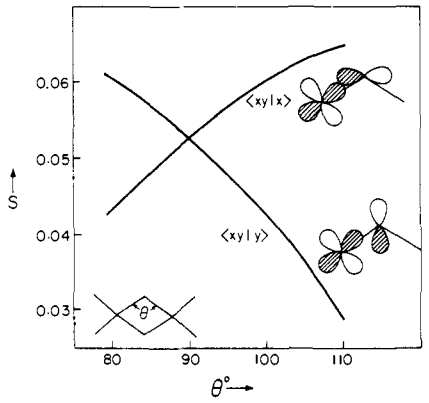

Figure 4. Variation of metal-ligand overlap S in a dibridged dimer geometry.

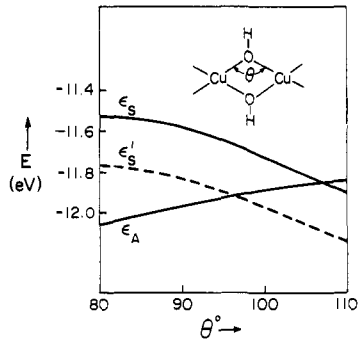

Figure 5. Energies of highest metal orbitals in $Cu_2(OH)_2Cl_4^{2-}$ as a function of bridge angle. The solid ϵ_S line is for an oxygen 2s Slater exponent of 2.275, the dashed ϵ_S line for a higher exponent of 2.7. The ϵ_A line does not depend on the oxygen 2s exponent.

(93°) were fixed as θ was varied while maintaining D_{2h} symmetry. Hückel parameters were taken from a model $[CuCl_2(OH)_2]^{2-}$ calculation (see Appendix 2). For this d^9 system we need again focus only on the two highest d-like MO's—ϕ_A and ϕ_S, shown in **6** and **7**. In this coordinate system the metal orbitals will remain xy for all M-L-M bridge angles since these are the only d orbitals of b_{1g} and b_{2u} symmetry. (There is an unimportant admixture of $4p_y$ component into the metal orbitals.) On the bridging atoms there is one symmetry adapted combination of p orbitals ($y_1 + y_2$) which interacts with ϕ_S and another combination ($x_1 - x_2$) which interacts with ϕ_A; the 2s oxygen orbitals can interact with ϕ_S but not with ϕ_A.

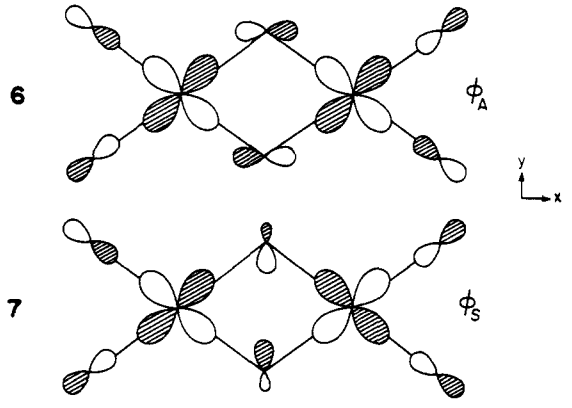

The relative order of ϵ_S and ϵ_A as a function of θ will be determined by the metal-bridging ligand overlap, especially the 2p orbitals since they lie much higher in energy (−15.6 eV) than the 2s (−32.2 eV). For $\theta = 90°$ (Figure 4) since the $\langle xy|x\rangle$ and $\langle xy|y\rangle$ overlaps are equal, one should expect ϵ_S to equal ϵ_A and a ferromagnetic coupling to occur. As θ increases, the overlap—and hence the *antibonding* character of the predominantly metal-like orbitals—with xy_A increases and the overlap with xy_S decreases. This would in turn lead to an increase in ϵ_A and a decrease in ϵ_S for $\theta > 90°$. Thus a larger AF coupling would be expected as the quantity $\epsilon_A - \epsilon_S$ increases. In Figure 5 the calculated results do indeed show ϵ_A rising and ϵ_S falling as θ increases, but that the crossing occurs not at 90° but somewhat later ($\theta \sim 107°$).

The preceding analysis ignored the effect of the 2s bridge orbitals, however, which also have an antibonding interaction with ϕ_S. This interaction would shift ϵ_S to higher energy and thus displace the crossing point to larger θ. In Figure 5 we illustrate the effect of a reduced $\langle xy|2s\rangle$ interaction where we have increased the 2s orbital exponent from 2.275 to 2.7. The net result is a downward shift in ϵ_S and the crossing occurs for $\theta = 96°$.

Table I. Experimental Cu–OH–Cu Bridging Angles (θ) and Singlet–Triplet Energy Differences ($2J = E_S - E_T$)(Values are taken from ref 27)

Compound	θ	$2J$(cm^{-1})
$[Cu(tmen)OH]_2Br_2$	104.4	−509
$[Cu(teen)OH]_2(ClO_4)_2$	103.0	−410
β-$[Cu(DMAEP)(OH)]_2(ClO_4)_2$	100.4	−201
$[Cu(EAEP)OH]_2(ClO_4)_2$	99	−130
$[Cu(bipy)OH]_2(SO_4)\cdot 5H_2O$	97	+48
$[Cu(bipy)OH]_2(NO_3)_2$	95.6	+172

Since favorable AF coupling depends only on the absolute value and not the sign of $\epsilon_S - \epsilon_A$, a ground state singlet should also occur for *smaller* values of θ below the cross-over point. For bridging angles smaller than 90°, the M-M direct overlap begins to be appreciable, and direct interaction can also lead to a ground state singlet.

We do not wish to ascribe much significance to the actual computed bond angles where the cross-over from a triplet to singlet ground state occurs, since the value is dependent on the choice of exponents. Nevertheless, these results are in very reasonable accord with the experimental results of Hatfield, Hodgson, and coworkers,[27] who have carefully characterized a series of OH-bridged Cu dimers with regard to their crystal structures and magnetic properties (see Table I). In these complexes the terminal groups are amine derivatives and in most cases there is a fifth group weakly coordinated to the Cu in an axial position. The Cu ions still have pseudo-square planar symmetry in this series, and the spin state is determined by the bridging ligands, so that the results of our simple model calculations can still be compared. The experimental results show $J > 0$ (triplet below singlet) for $\theta < 98°$ and $J < 0$ and growing in magnitude for larger θ. This suggests that our latter choice of parameters is in better agreement with experiment. Although no complexes have been reported with $\theta < 95°$, it would be of interest to observe whether the singlet state would eventually become the ground state again as indicated by our calculations.

This analysis has focused on the numerator $|\epsilon_S - \epsilon_A|^2$ of the AF contribution (eq 8), since the denominator is slowly varying. Actually $J_{aa} - J_{ab}$ will be decreasing slightly as θ increases since $J_{ab} \sim 1/R$—resulting in enhancement of the singlet-triplet gap. We also note at this point that the symmetry of the bridging group orbitals as a significant factor in determining the magnetic properties of dimers has been stressed by Bertrand.[28]

The Role of Other Geometrical Distortions

The Twisting Mode in $Cu_2Cl_6^{2-}$. A related series of compounds,[29-37] all containing the $Cu_2Cl_6^{2-}$ entity, has been

Table II. Experimental Exchange Parameters and Structural Information for Dimers Containing the $[Cu_2Cl_6]^{2-}$ Unit

Compound	Bond angles[a]			R(Cu-Cu)(A)	$2J$ (cm^{-1})	Ref
	Cu-Cl_b-Cu	Cl_t-Cu-Cl_b	Cl_t-Cu-Cl_t			
$LiCuCl_3 \cdot 2H_2O$[b]	95.1	180	93	3.47	(<0)	30
$KCuCl_3$[b]	95.9	174.5	93.2	3.44	−39	31
$(CH_3)_2NH_2CuCl_3$[b]	95.6	166	92.3	3.42	−3	32
$Ph_4AsCuCl_3$	93.6	145	100.3	3.39	+46	29
Ph_4PCuCl_3	93.3	144	100.9	3.36	[c]	33

[a] Key: Cl_b = bridging Cl, Cl_t = terminal Cl. Cl_t-Cu-Cl_b refers to the larger of two such angles. Where a range of angles was observed, the average is given in the table. [b] These compounds show varying degrees of association of the dimers to infinite network structures. [c] Not known.

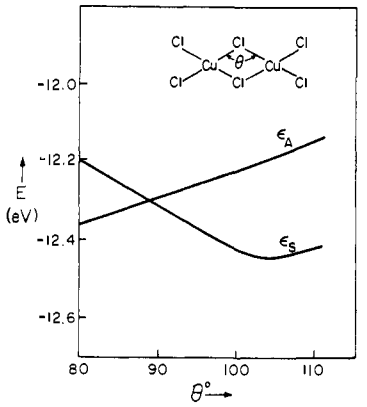

Figure 6. Energies of highest metal orbitals of $Cu_2Cl_6^{2-}$ as a function of bridge angle.

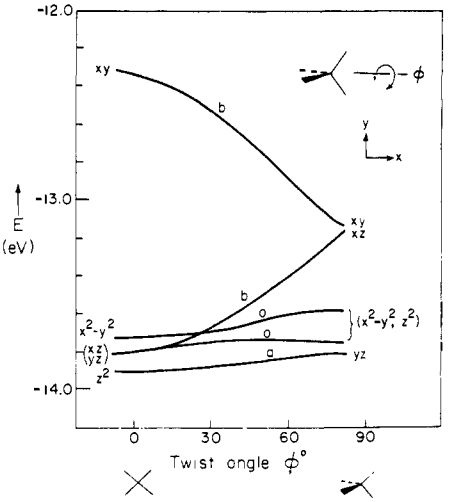

Figure 7. Energies of metal orbitals of $CuCl_4^{2-}$ as a function of dihedral twist angle.

found to display both singlet and triplet ground states depending upon the geometry when various counterions are used (see Table II). The bridging Cu-Cl-Cu angles are all rather similar ($\theta \approx 95°$), although the one compound with the triplet ground state has a slightly smaller angle (93.6°) than the rest. In addition the central Cl atoms in the latter compound are twisted out of the molecular plane, **8**, with

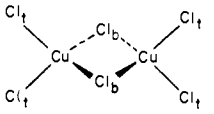

8

resulting Cl_b-Cu-Cl_t angles far from coplanar.[29]

We have investigated the effects of the bending and twisting modes on superexchange in the $Cu_2Cl_6^{2-}$ species, with parameters obtained from model $CuCl_4^{2-}$ calculations described in Appendix 2. The level ordering of the two highest metal orbitals (xy-like), shown in Figure 6, is essentially the same as the OH-bridged series—a larger AF coupling expected as θ increases from 90°. The antisymmetric orbital, ϕ_A, lies higher in energy than ϕ_S for $\theta > 90°$ because of the greater interaction of xy with the $3p_x$ orbital relative to the $3p_y$ orbital of chlorine.[34] An earlier MO description of $Cu_2Cl_6^{2-}$, given by Willett and Liles,[35] is in qualitative agreement with our analysis.

In our study of the twisting mode the plane containing the Cu atoms and the bridging chlorines was rotated by an angle, ϕ, relative to the plane of the terminal ligands. The following structural parameters were used: R(Cu-Cl_b) = 2.3, R(Cu-Cl_t) = 2.26, Cl_b-Cu-Cl_b angle = 85°, Cl_t-Cu-Cl_t angle = 93°, and $0 \leq \phi \leq 90°$. To understand what happens in the dimer it is best to consider the effect of a similar distortion on a $CuCl_4^{2-}$ monomer with similar structural parameters. This is done in Figure 7. The molecule is transformed from C_{2v} symmetry (very nearly D_{4h}) for $\phi = 0°$, through C_2, to C_{2v} symmetry again (very nearly D_{2d}) for $\phi = 90°$. The xy orbital containing the unpaired electron, while widely separated from the others for $\phi = 0°$, becomes essentially degenerate with the xz orbital in the perpendicular geometry. Only the region $0° \leq \phi \leq 50°$ will concern us since the known compounds fall into this area. For intermediate values of ϕ, xy and xz both have b symmetry, and the xy orbital incorporates xz character to lie in the plane midway between the Cl_t-Cu-Cl_t and Cl_b-Cu-Cl_b planes, **9**.

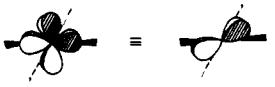

9

In the dimer (Figure 8) the xy orbitals are split into ϕ_S and ϕ_A, with ϕ_A higher in energy for planar $Cu_2Cl_6^{2-}$, as we would expect for a bridge angle of 95° from our previous discussion. As the molecule is twisted, a level crossing occurs near $\phi = 35°$ where a ferromagnetic coupling would arise. This is in agreement with the observation that the dimer with a substantial twist angle (48° between dihedral planes) has a triplet ground state.

The origin of this crossing can be traced as follows. In the MO ϕ_A (**10**) the xy-x overlap is decreasing as the bridge atom is lifted out of the molecular plane (**12**). The formerly "pure" xy orbital no longer points directly at the bridge atoms but now lies midway between the original plane and the Cl_b-Cu-Cl_b plane. (The coordinate system in **12** has been rotated to show this effect more clearly.) In the ϕ_S MO, **11** → **13**, the situation is similar since the xy-y overlap is also decreasing, but in the twisted geometry it can also interact with z to compensate partially for this loss and to account for the smaller slope of ϵ_S as a function of ϕ. Finally we note that at the special perpendicular D_{2h} geome-

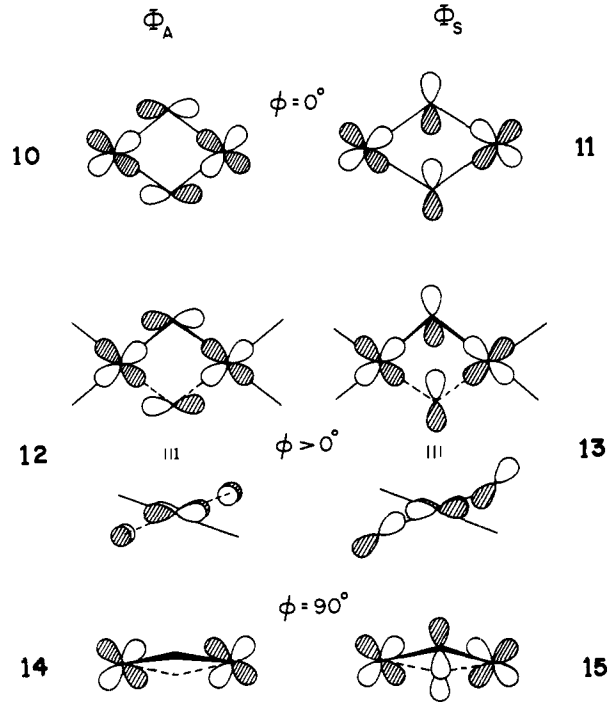

try (compared with C_{2h} for intermediate points) ϕ_A has *no* bridge atom component (**14**) while ϕ_S retains z character (**15**) and is pushed to higher energy. In summary both an increase in twist angle ϕ and decrease in bridge angle θ would lead to smaller exchange couplings.

Before leaving the subject of doubly bridged dimers we should direct the reader to two elegant discussions of the factors influencing the bridging angle.[36,37]

Dimeric Structures with Pentacoordinate Metal Centers. There are a number of structural[38-42] and magnetic[40,43] studies of pentacoordinate Cu(II) dimers. These show a variety of structures in which the local geometry about each Cu is square pyramidal (SP) or trigonal bipyramidal (TBP).[44] Species have been found with one or two bridging groups. We shall focus here on but one possible distortion of a dimer with a single group bridging two pentacoordinate Cu atoms.

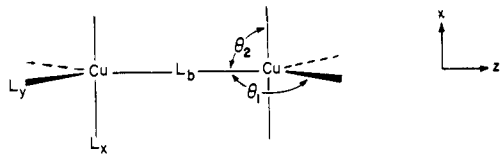

16

Examples of such species include a Cl-bridged and a CN-bridged Cu dimer where the terminal ligands in both cases are amine derivatives.[38] Our model for this study is the hypothetical $[(Cl_4Cu)\text{-}Cl\text{-}(CuCl_4)]^{5-}$ molecule where all Cu-Cl bond lengths are taken to be 2.3 Å, and the angles between the bridging Cl and terminal Cl's in the respective y and x planes are θ_1 and θ_2. Two possible distortions are considered. (a) $\theta_2 = 90°$, θ_1 varied from 90 to 130°. This transforms the SP dimer ($\theta_1 = 90°$) through the TBP dimer ($\theta_1 = 120°$). (b) $\theta_1 = \theta_2$, θ_1 varied from 90 to 130°. This changes the axial-metal-basal angle of a SP dimer.

The Cl-bridged example mentioned above corresponds to (a) with $\theta_1 = 121, 124°$ and the CN-bridged example corresponds to (b) with $\theta_1 = 113°$. In addition the axes of the TBP's are rotated 90° relative to each other, but the results of our model should still pertain. Our calculations are illustrated in Figures 9 and 10.

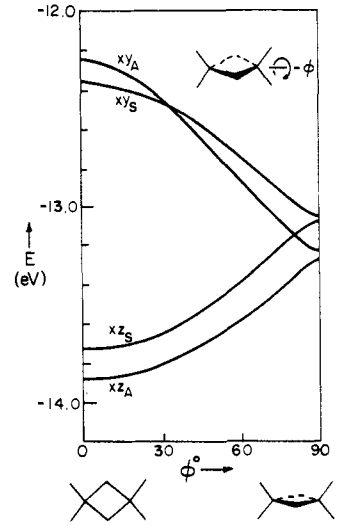

Figure 8. Energies of selected orbitals in $Cu_3Cl_6^{2-}$ as a function of dihedral twist angle of bridging atoms.

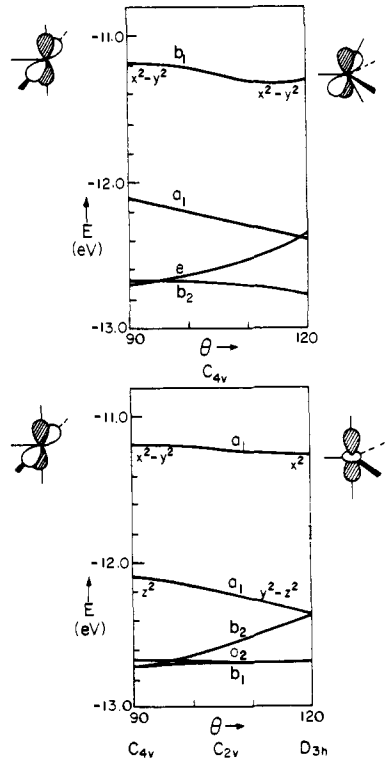

Figure 9. $CuCl_5^{3-}$ levels: top, square pyramidal distortion, maintaining C_{4v} symmetry; bottom, distortion toward trigonal bipyramid C_{4v} (θ = 90°) → C_{2v} → D_{3h} (θ = 120°).

In the $CuCl_5^{3-}$ fragment, as the four basal ligands are bent back, the highest orbital remains $x^2 - y^2$ (b_2). This is if C_{4v} symmetry is maintained, as in mode (b). If only two ligands are bent back, in the resulting C_{2v} symmetry the z^2 and $x^2 - y^2$ orbitals will mix. The $x^2 - y^2$ orbital acquires components along the z axis and eventually becomes the "x^2" orbital (a_1') of the D_{3h} TBP. The z^2 orbital in turn becomes the lower-lying "$y^2 - z^2$" member of the e_1' pair.

In the case of the dimer with $\theta_1 = \theta_2 = 90°$ there are *no* bridging orbitals on the ligand which have the proper symmetry to interact with *either* of the symmetric (ϕ_S) or (ϕ_A) $x^2 - y^2$ orbitals (b_{1g} and b_{1u} in D_{4h} symmetry). Hence no AF coupling would arise due to through bond coupling since $\epsilon_S = \epsilon_A$. The situation remains the same in case b where

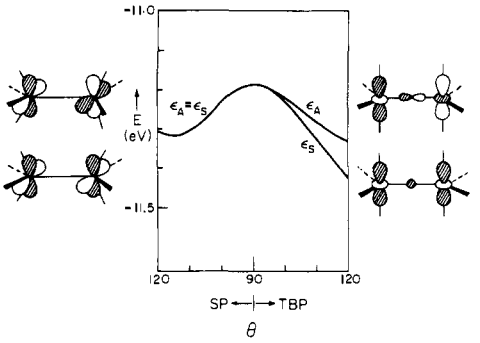

Figure 10. Monobridged $Cl_4CuClCuCl_4$ dimer showing distortions of fragments toward SP and TBP.

local C_{4v} symmetry is maintained, so that there should be essentially no superexchange interaction for such geometries.

To the extent that z^2 is admixed in the C_{2v} case, however, interactions are possible with the filled $3p_z$ and 3s Cl orbitals. Since the higher-lying p orbitals interact more strongly with the d orbitals, ϕ_A increases in energy relative to ϕ_S as θ_2 increases and a singlet should be stabilized (Figure 10).

This accounts for the large coupling (-144 cm^{-1}) observed for the Cl-bridged case, where $\theta = 121°$ and no interaction would have been expected for $\theta = 90°$. Unfortunately the small interaction in the CN bridged (-5 cm^{-1}) cannot be traced solely to the fact that the d orbital is purely $x^2 - y^2$. Cl^- had the property that the orbitals capable of interacting with the S and A d combinations were very different in energy and thus effective in splitting the d-like MO's. The two highest lone pair orbitals of CN^- are much closer in energy and would be less effective in producing an $\epsilon_S - \epsilon_A$ energy gap.

Influence of Substituents on Superexchange Interactions

In the preceding discussion we were attempting to analyze how geometrical distortions of a particular dimer affected the order and spacing of the highest occupied MO's containing the unpaired electrons. Here we shall focus on these same metal orbitals for a fixed geometry as a function of the changes in the bridging ligands.

Electronegativity Effects. From second-order perturbation theory the quantity of interest $\epsilon_S - \epsilon_A$ is given by

$$\epsilon_S - \epsilon_A = \frac{|H_{ld}^S|^2}{\epsilon_d - \epsilon_{lS}} - \frac{|H_{ld}^A|^2}{\epsilon_d - \epsilon_{lA}}$$

The labels l and d stand for bridging ligand and metal d orbitals, respectively. In the above expression it is assumed that there is only one important ligand orbital of each symmetry (A and S). Furthermore

$$H_{ld}^S = \langle \phi_d^S | H | \phi_l^S \rangle = \sum_i C_{il}^S \langle \phi_d^S | H | \chi_i \rangle$$

where the χ_i are the atomic orbitals comprising the ligand orbital. Usually the M-L interaction will be dominated by the interactions with the orbital(s) of the atom nearest the metal, χ_0

$$H_{ld}^S \approx C_{0l}^S H_{0d}^S$$

which leads to the following expression

$$\epsilon_S - \epsilon_A = \frac{(C_{0l}^S)^2 (H_{0d}^S)^2}{\epsilon_{dS} - \epsilon_{lS}} - \frac{(C_{0l}^A)^2 (H_{0d}^A)^2}{\epsilon_{dA} - \epsilon_{lA}}$$

One way in which substituents on the bridging ligand can affect the coupling between metal ions is to increase the amplitude C_{0l} of the orbital χ_0 nearest the metals so as to increase the metal-ligand interaction. In the cases with which this analysis is concerned, the amplitudes in ϕ_l will not be changing appreciably, but the *total* charge on the bridging ligand *will* be changing and will affect primarily the denominator of the expression.

In the self-consistent charge process (or in any other method using a self-consistent field approach), removal of electron density from an atom reduces the electron-electron repulsion and lowers the atomic orbital levels of that atom. This in turn will lead to lower orbital energies in MO's which contain substantial character of the atom involved.

Consider what happens when the ligands involved in the important ligand orbitals ϕ_l^S and ϕ_l^A are made more *positive* and their orbital energies ϵ_{lS} and ϵ_{lA} are *lowered* to $\epsilon_{lS} - \Delta$ and $\epsilon_{lA} - \Delta$, respectively ($\Delta > 0$). The metal orbitals now differ in energy by an amount

$$\epsilon_S' - \epsilon_A' = \frac{|H^S|^2}{\epsilon_d - \epsilon_{lS} + \Delta} - \frac{|H^A|^2}{\epsilon_d - \epsilon_{lA} + \Delta}$$

$$\approx \epsilon_S - \epsilon_A - \Delta\left[\frac{|H^S|^2}{(\epsilon_d - \epsilon_{lS})^2} - \frac{|H^A|^2}{(\epsilon_d - \epsilon_{lA})^2}\right]$$

Since the quantity in brackets is positive, $\epsilon_S' - \epsilon_A' < \epsilon_S - \epsilon_A$ and the *antiferromagnetic interaction decreases as electron density is removed from the bridging atoms.* Conversely, an *increase* in electron density raises the ligand levels and *enhances* the AF coupling. This conclusion was also reached by Hodgson, Hatfield, and their coworkers.[45]

To illustrate this effect the model complex **17** has been

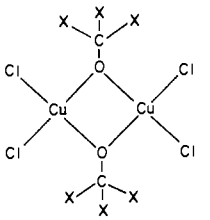

17

studied as the electronegativity of X is varied. In one case X has been chosen as a hydrogen whose orbital energy has been steadily decreased from -13.6 to -17.6 eV, to simulate an increase in electronegativity. The substituent $-CH_2Cl$ has also been used to replace $-CH_3$ by a more electron-withdrawing group. The parameters for the dimer were obtained from calculations on the square planar $[Cl_3CuOCX_3]^{2-}$ species with $R_{Cu\text{-}Cl} = 2.26$, $R_{Cu\text{-}O} = 1.94$ Å. Separate calculations were also performed on the isolated ligand X_3CO^- in the presence of a +1 point change.

In both series of calculations the resulting orbital levels H_{ii} of the oxygen 2s and 2p orbitals become lower in energy as X is made more electronegative. In the calculation on the Cu monomer, the 3d levels also shift downward, but there is an overall increase in the gap between metal and ligand levels. The increased energy gap as electron density is withdrawn from the bridging ligands is reflected in the decreasing $\epsilon_A - \epsilon_S$ splitting in the xy-like metal orbitals. The electronic structure of the bridge is essentially identical with the OH-bridged series discussed earlier, since the $2p_x$ and $2p_y$ lone pair orbitals of the O in the methoxy group differ little from the OH species. For an assumed Cu-O-Cu bridge angle of 90°, ϕ_A lies slightly higher in energy than ϕ_S, and the splitting decreases from 0.104 to 0.067 eV as the "dummy" atom is made more electronegative; a similar reduction (of 0.011 eV) is observed when H is replaced by Cl.

Acetate-Bridged Dimers. Historically antiferromagnetic coupling in a dimer compound was first observed in the acetate-bridged molecule $Cu_2(CH_3COO)_4 \cdot 2H_2O$,[46,47] and a

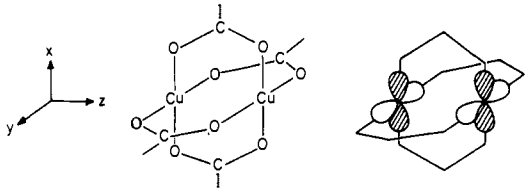

18

variety of related dimers have been reported which possess the common O-CR-O triatomic molecular bridge.[3,48] Although the nature of the electronic structure has been a matter of considerable controversy,[1,10,48,49] it is now evident that the unpaired electron on each Cu occupies a $x^2 - y^2$-like orbital oriented toward the four O atoms in the very nearly square-planar environment about the metal.[50] For a Cu-Cu distance of 2.64 Å the small δ–δ overlap would preclude any direct interaction. The symmetric and antisymmetric $x^2 - y^2$ orbitals, d_S and d_A (Figure 11), can interact, however, with the symmetry adapted combinations of lone pair acetate orbitals, l_S and l_A. In the SCC-EHT calculations on CH_3COO^- the highest occupied MO's are the $a_1(l_S)$, $b_2(l_A)$ and $a_2(\pi)$ orbitals shown below.

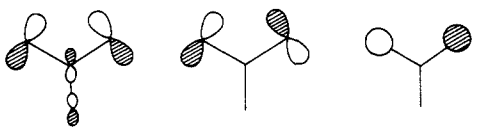

19 l_S **20** l_A **21** π

Despite the favorable through-space interaction in l_S it is pushed higher in energy than l_A, presumably because of the antibonding interaction with the C-C bonding orbital.[12] If both orbitals have nearly equal overlaps with the $x^2 - y^2$ orbitals, the higher-lying S orbital would be expected to produce the ordering $\phi_S > \phi_A$ for the metal orbitals of the dimer. In Figure 11, which shows the results for the formate bridged dimer, the ordering $(x^2 - y^2)_S$ (−12.73) > $(x^2 - y^2)_A$ (−12.84) is found and this order is retained in the acetate series to be discussed below.[51] That differential interaction with the acetate groups will produce a splitting of the Cu orbitals has been previously pointed out by Goodgame, Skapski, and coworkers.[52]

If our calculations are correct, not only is there no δ bond in the copper carboxylate dimers but there may be somewhat of a δ antibond. What we mean by this is the following. The singlet ground state of the system will be a mixture of the two configurations $\psi = c_S(S)^2 + c_A(A)^2$ where S = $(x^2 - y^2)_S$, A = $(x^2 - y^2)_A$. With A and S close in energy c_S and c_A will be comparable size. To the extent that A is below S in energy the net effect will be slight metal-metal antibonding. Of course at very short Cu-Cu separations the direct interaction will begin to dominate, bringing S to lower energy, but in the distance range in question the indirect coupling is greater. No direct proportionality between the magnitude of AF coupling and Cu-Cu distance is to be expected. The experimental facts are that the coupling in the formate dimer is greater than in the acetate, despite a shorter Cu-Cu separation in the latter.[52] In $Cu_2(CH_3CO_2)_4$(pyrazine) the copper atoms are 2.58 Å apart[53a] and yet the coupling is, for copper carboxylates, moderate.[53b] In this complex the Cu-Cu separation at 100 K is only 0.007 Å shorter than at 300 K.[53a]

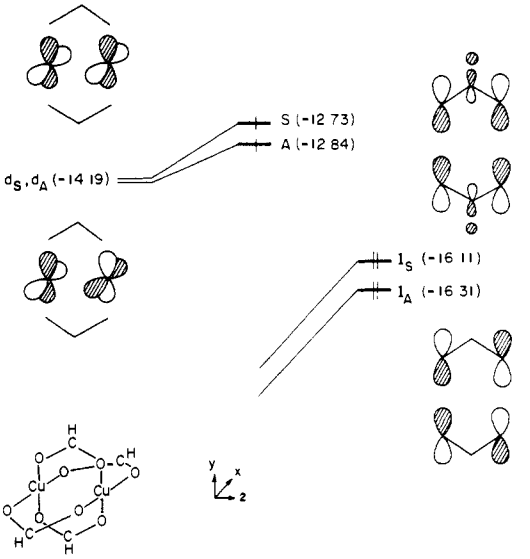

Figure 11. Selected metal and ligand lone pair orbitals in $Cu_2(HCOO)_4$ interacting.

Table III. Effect of Electronegativity Changes in the O-CX-O Bridged Cu Dimer Series (X = H, CH_3, and CCl_3)

		CH_3			
			$H_{ii}(H)$ =		
	H	13.6	15.6	17.6	CCl_3
$H_{ii}(2p_O)$	−16.64	−16.59	−16.89	−17.12	−17.30
q(O)	−0.699	−0.727	−0.721	−0.715	−0.724
ϵ_S (eV)	−12.733	−12.711	−12.737	−12.755	−12.754
ϵ_A (eV)	−12.843	−12.836	−12.853	−12.864	−12.869
$\epsilon_S - \epsilon_A$ (eV)	0.110	0.125	0.116	0.109	0.115
$2J$ (cm^{-1})[52]	−485	−305			
μ_{eff} (μ_B)[3]		1.39			1.77
pK_a(L)	3.75	4.75			0.70

The effect of electron-withdrawing groups on the Cu-Cu interaction in the acetate series was probed by calculations on $(O\text{-}CX\text{-}O)^-$ bridged compounds where X = H, CH_3 (with the IP of H variously set at 13.6, 15.6, and 17.6 eV), and X = CCl_3.

The results (Table III) again show a *reduced* Cu-Cu interaction as the H is made *more electronegative* or is replaced by Cl, in agreement with the experimental observation that replacement of CH_3 by CCl_3 reduces J and increases the effective magnetic moment from 1.39 to 1.77 μ_B.[3,48a] Formate is somewhat anomalous since the calculations show a reduced O charge and a reduced Cu-Cu interaction (consistent with the greater acidity of formate) compared to acetate. The experimental coupling[52] is actually greater in formate ($2J$ = −485 cm^{-1}) than in acetate (−305 cm^{-1}). Although these calculations are only to be semiquantitative at best, a possible explanation may lie with the shorter Cu-O bond lengths (1.983 Å) in the formate dimer than in the acetate dimer (2.03 Å). (These structural and magnetic data relate to the $[(Me_4N)_2][Cu(X\text{-}CO_2)_2(NCS)_2]_2$ molecules.[52] In our calculations the basic structure was taken from a recent neutron-diffraction study[54] of $[Cu(CH_3COO)_2(H_2O)]_2$, and standard bond lengths were assumed for ligand substituents.) We should bring to the reader's attention a recent structural and magnetic study of a copper trifluoroacetate quinoline adduct.[48b] The magnitude of the Cu-Cu interaction in the trifluoroacetate derivative ($2J$ = −310 cm^{-1}) is very similar to

that in the acetate. This brings into question the correlation between the substituent electron withdrawing power and the metal-metal coupling.

Though we have not carried out any relevant calculations, we should mention at this point two interesting systems related to the copper acetates. The first of these are the triazenido ($RNNNR^-$) complexes of Cu and Ni, exemplified by $Cu_2(Ph_2N_3)_4$. These possess a geometry similar to the acetates, but with a much shorter metal-metal distance.[55a] There is a corresponding strong antiferromagnetic coupling.[55b] The other set of molecules are the strongly coupled d^4-d^4 systems of the type $M_2(RCO_2)_4$, M = Cr or Mo.[56] In these compounds the question of thermal population of a high spin state does not arise—indeed the short M-M bond distance is indicative of metal-metal multiple bonding.

The orbital interaction diagrams discussed so far have always dealt with stabilization of a low-spin ground state as caused by *destabilization* of metal orbitals by filled ligand orbitals. The pyridine *N*-oxides, discussed in the next section, may provide a situation where stabilization by low-lying virtual orbitals influences the quantity $\epsilon_S - \epsilon_A$.

Pyridine *N*-Oxide Dimers. The pyridine *N*-oxide (pyO) bridged Cu dimers have been studied extensively with regard to magnetic properties.[57-59] One of the typical dimeric units resembles the OH-bridged dimers,[60] e.g., **22**, with a

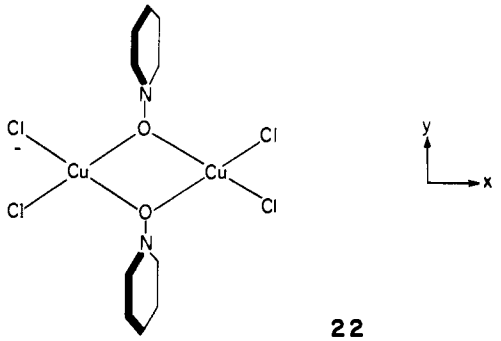

22

Cu-O-Cu bridging angle of 108°. The pyridine rings, nearly perpendicular to the Cu_2O_2 plane, are twisted 70° about the N-O bond out of that plane, and the terminal Cl ions are also somewhat puckered out of the ring plane. An idealized structure was adapted from the experimental geometry so that all atoms bonded to the Cu are kept in the same plane and the pyridine rings are rotated perpendicular to this plane.

Charge iterative calculations on the pyO molecule itself showed the highest filled orbitals to be localized primarily on the oxygen

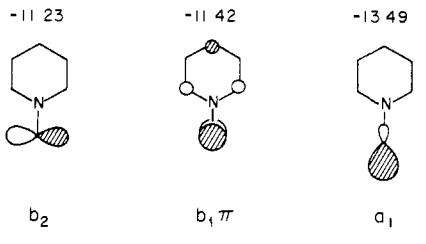

When the plane of the ring is perpendicular, the b_1 and a_1 orbitals can interact with the A and S combinations of the *xy* metal orbitals, respectively. The situation is strongly reminiscent of the OH-bridged series since the A and S ligand orbitals are essentially *x* and *y* oxygen orbitals. The large bridging angle would lead to a strong preference for an ordering $\epsilon_A > \epsilon_S$ based on our earlier overlap analysis. The location of the ligand S orbital below the ligand A orbital would reinforce this tendency, and in fact this ordering was borne out by the calculations.

The experimentally observed splittings in the pyO series (~1000 cm^{-1}) are among the largest observed in any dimer and yet still small enough to have a triplet population detectable by standard techniques. It would appear that a primary factor in the coupling is the large Cu-O-Cu bond angle, since a coupling of -500 cm^{-1} was observed in the OH-bridged series with a smaller (105°) angle. An assessment of the effects of substituents would be aided by further systematic studies on the structures of these dimers.

Metal-Metal Interactions in Oxalate and Squarate Dimers

One final class of dimeric compounds will be treated, which strikingly shows how superexchange interactions can be decomposed into pairs of MO contributions. In the oxalate-bridged compounds a pseudo-octahedral metal ion is bridged by an oxalate moiety which serves as two bidentate ligands. Structures and magnetic susceptibility measurements have been reported for the Cu(II) and Ni(II) compounds, as well as for a squarate, **24**, bridged Ni dimer.[61-63]

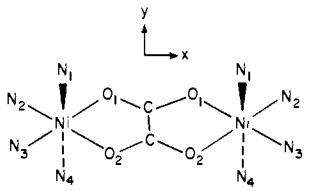

23

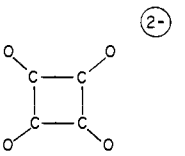

24

The Cu oxalate structure is considerably distorted from octahedral symmetry, with N_3 replaced by an O ligand with much longer bond length and with significant lengthening of the $Cu-O_1$ bond as well.

In the above coordinate system the unpaired Ni electrons will occupy the z^2 and *xy* orbitals, while for Cu the stronger N-ligands of the idealized structure would be expected to orient the unpaired electron along the N_1-N_4 axis in the z^2 orbital. AF exchange is observed in the Ni compounds (-17 cm^{-1} in $C_2O_4^{2-}$ and -1 cm^{-1} in $C_4O_4^{2-}$) while none is observed for Cu.

Our analysis in the theoretical section and in Appendix 1 showed that in such a case with two unpaired electrons on each metal atom, the superexchange could be decomposed into a sum of two contributions—one proportional to the splitting $[\epsilon(z^2_S) - \epsilon(z^2_A)]^2$ and another proportional to $[\epsilon(xy_S) - \epsilon(xy_A)]^2$, where the symmetry adapted combinations of metal orbitals are sketched in Figure 12. The four lone pair orbitals of $C_2O_4^{2-}$ are also shown and are labeled as l_{z^2S}, l_{z^2A}, l_{xyS}, and l_{xyA} to denote with which particular metal orbital combination each can interact.

The qualitative level ordering of the oxalate orbitals[64] follows the expected trend from nodal structure with $xy_A > xy_S$, but the orbital with best O-O overlap (z^2_S) lies above the z^2_A orbital. This is apparently a result of through bond coupling,[12] since the former orbital will be shifted to higher energy by virtue of its antibonding interaction with the C-C bonding orbital.

The ordering of the pairs of metal orbitals of the dimer follows the ordering of ligand levels: z^2_S (−11.82) > z^2_A (−11.85) and xy_A (−12.04) > xy_S (−12.17). (The relative ordering of the z^2 and *xy* pairs is determined by the ligand field about the metal.) The smaller z^2 splitting (0.03 eV) compared to *xy* (0.13 eV) can be attributed to the much more favorable *xy*-ligand overlap, since the z^2 orbitals are oriented along the perpendicular axis. This is also consonant with the stronger AF coupling in the Ni dimer than in

the Cu dimer where the xy orbitals are filled and cannot contribute to superexchange.

The analysis of the squarate system—where the same H_{ii} parameters and bond distances are used as in the oxalate system—is quite similar except that the ligand orbitals, shown in **25** → **28**, now have the ordering $z^2_S > z^2_A$ and

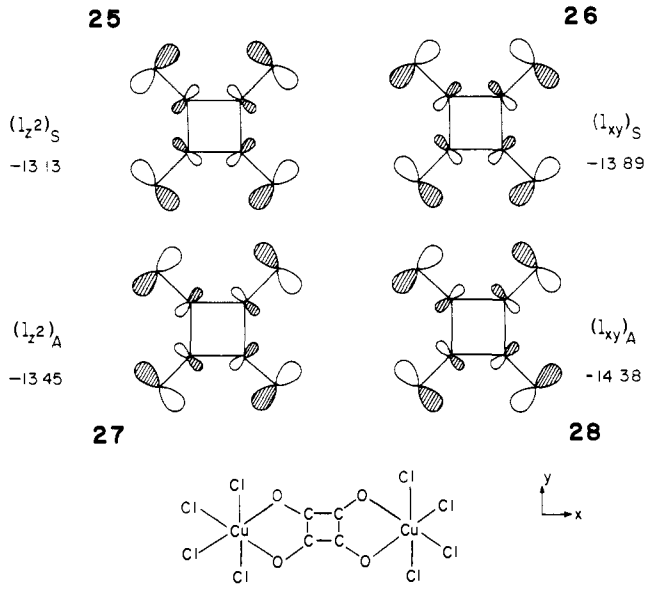

$xy_S > xy_A$. The ligand z^2_S orbital has a strong antibonding interaction with the highest C-C bonding orbital of the cyclobutane system,[65] and xy_A is markedly stabilized by an interaction with the lowest σ^* orbital of the C-C system. This ordering is again reflected in the final metal orbitals' energies, with a z^2 energy difference of 0.05 eV and a difference of 0.12 eV for xy. That the squarate interaction is observed to be extremely small (ca. -1 cm^{-1}) experimentally is presumably due to the fact that the self-consistent orbitals of the larger $C_4O_4^{2-}$ system would be lower in energy and interact more weakly with the metal orbitals, as our previous electronegativity studies would argue. The main points of these arguments—the occupancy of z^2 vs. xy, better xy-ligand overlap, and weaker squarate-metal interaction—were initially forwarded by Duggan and Hendrickson[63] and their suggestions have apparently found some support from these calculations. Since the structure for the squarate dimer has not yet been determined, the small interaction may be due to distortions from the assumed geometry.

Metal-Metal Interactions and through Bond Coupling

In the realm of organic chemistry photoelectron spectroscopy has provided abundant evidence for the splitting of lone pair and π levels as a consequence of interaction with occupied and empty σ levels.[12] The discussion of the previous sections is much along the same lines—the bridging group provides orbitals of a certain symmetry type, and this in turn effects a certain well-defined splitting of the metal orbitals.

An interesting point is that among these metal-metal coupled systems that have been carefully studied there are few examples of the coupling unit which has proven most spectacular in organic systems—two lone pairs separated by three σ bonds. The unit is exemplified by 1,2-diaminoethane **29**, pyrazine **30**, and diazabicyclo[2.2.2]octane (DABCO) **31**. The through bond coupling of the N lone pairs in these molecules is large, producing splittings between symmetric and antisymmetric lone pair combinations of 1-2.5 eV. The interaction which leads to these large

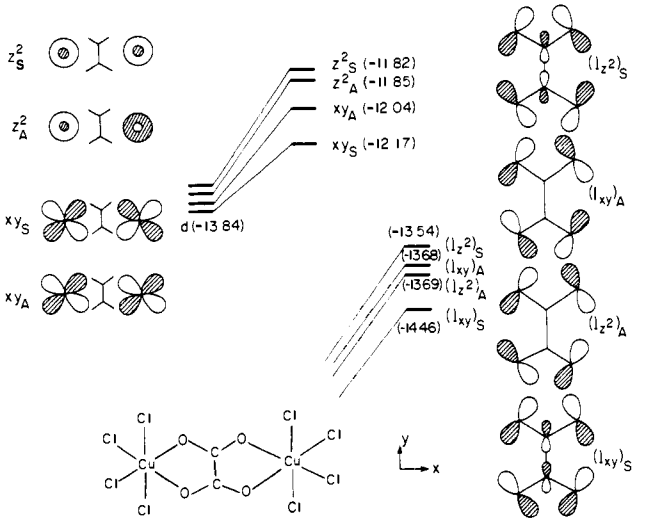

Figure 12. Interaction diagram for selected metal and ligand lone pair orbitals in the oxalate bridged Cu dimer.

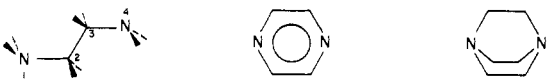

splittings has a strong conformational dependence, in the prototype **29** being relatively insensitive to rotation around the central (2-3) σ bond, but very sensitive to torsion around the side (1-2, 3-4) bonds. Metal centers coordinated to such systems should respond to the energy splitting by showing a sizable antiferromagnetic coupling.

The kind of molecule we have in mind is shown in **32** or **33**. These appear to be unrealistic, but we would encourage

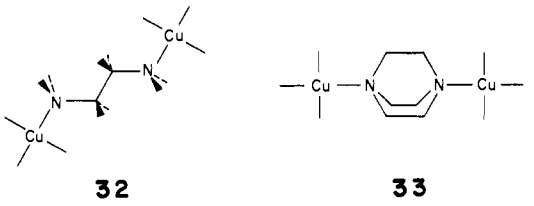

experimental investigation of this general type of complex. Ethylenediamines generally prefer to act as bidentate ligands toward one metal center rather than bridging two metal atoms. A unique structure, $Cu_2EDTA{\cdot}4H_2O$ has the EDTA molecule bridging in an extended fashion two Cu(II) atoms.[66,67] A preliminary study shows very little decrease at low temperatures in the magnetic moment from its 1.92 μ_B value at 295°K.[68] This unfortunately is consistent with the solid state geometry, the N-Cu directions, when viewed along an N-C bond, forming an angle of 72° with the crucial coupling CC bond.

Several DABCO-copper(II) complexes are known: $Cu(acetate)_2{\cdot}0.5DABCO$,[69a] $CuCl_2{\cdot}DABCO$,[69b,c] $CuCl_2{\cdot}0.5DABCO$.[69c] In the acetate complex, which presumably retains the basic $Cu_2(acetate)_4$ structure, adding in the solid state bridging DABCO units, the unpaired electron is in an orbital which does not have the correct symmetry to interact with the through-bond coupled DABCO lone pairs. The $CuCl_2$ DABCO complexes show normal magnetic behavior.[69c] Their structures are unknown and would be of considerable interest.

Pyrazine has been utilized as a bridging ligand in several instances. The 1:1 copper nitrate:pyrazine complex shows

antiferromagnetic coupling between the Cu(II) ions separated by 6.7 Å.[70] The crystal structure contains infinite chains of $Cu(NO_3)_2$ alternating with pyrazine.[71] The nitrate groups are asymmetrically bonded, so that the local symmetry at the copper atoms is low. It is difficult to determine the precise orientation of the orbital holding the unpaired electron.[72] It should have considerable σ character (along the Cu-pyrazine axis) and thus this may be the kind of system where the through-bond coupling capability of the pyrazine is exhibited. The magnetic properties of several other pyrazine bridged copper, nickel, and cobalt systems have been examined.[73-79]

A pyrazine molecule has been used to bridge two octahedrally coordinated Ru or Os centers in varying oxidation states (2+, 2+; 3+, 2+; 3+, 3+) in the elegant studies of Taube and coworkers.[80] In these systems the pyrazine acts as a weak coupling unit through its π system. We think its effectiveness for mediating interaction between metal centers should be greater when it operates through its σ system, as in the d^9-d^9 systems.

Summary and Discussion

The preceding molecular orbital analysis has focused on the splitting in energy between the highest two orbitals—$|\epsilon_S - \epsilon_A|^2$—as the dominant factor in antiferromagnetic interactions of d^9 metal dimer complexes (see eq 7).

$$2J = 2K_{ab} - \frac{|\epsilon_S - \epsilon_A|^2}{J_{aa} - J_{ab}}$$

The computed changes in this quantity as a function of geometry have been found to reflect the experimental variations in J in hydroxo- and chloro-bridged Cu dimers. Although our intent has been the analysis of *qualitative* changes in the orbital levels, the calculated splittings (~0.1-0.2 eV) yield values for $2J$ (ca. -16 to -140 cm^{-1}) of reasonable magnitude (assuming $J_{aa} - J_{ab} \simeq 5$ eV).

For d^n systems the total superexchange interaction can be decomposed into contributions from disjoint sets of orbital pairs, $|\epsilon_i - \epsilon_j|^2$, and the various types of orbital interactions were reviewed for oxo-bridged metal dimers.

Although only the magnitude $|\epsilon_S - \epsilon_A|$ is important as far as superexchange is concerned, the actual relative ordering in most cases (with the possible exception of the acetate dimers) can be inferred from the calculations and the known experimental information. Since the levels have real physical significance, in the sense of observables, only for the high-spin state, which is usually not the ground state, experimental verification of the level scheme would be difficult. Information could possibly be obtained, however, from ESR experiments on the dimers where an electron has been added or removed from the system in order to tell whether the S or A level lies higher in energy.

Substituents have also been found to influence the $\epsilon_S - \epsilon_A$ splitting—increasing it (and hence the AF coupling) as electron density is added to bridging atoms, decreasing it as electron density is removed. Model calculations demonstrated the effect in methoxy- and acetate-bridged dimers.

One of the more interesting features to emerge from this analysis has been a means to analyze metal-metal interactions when the intervening ligand is a "complicated" polyatomic molecule. At least in the case of acetate, oxalate, and squarate dimers, inspection of the highest ligand orbitals of the proper symmetry to interact with the d orbitals has been sufficient to account for the ordering of the d levels in the dimer and their relative importance in superexchange.

Until recently there has been little theoretical foundation for analysis of superexchange in molecular dimers with polyatomic ligands. It has been attempted to create such a framework on which future quantitative developments may rest.

Table IV. Parameters for the Self-Consistent Charge Calculations. All Quantities Are in eV

Atom	C	B	A	γ
C 2s	19.50	12.07	1.54	10.201
2p	10.66	12.07	1.54	10.201
N 2s	25.50	13.64	2.01	11.052
2p	13.14	13.64	2.01	11.052
O 2s	32.40	15.00	1.72	13.625
2p	15.87	15.00	1.72	13.625
Cl 3s	25.3	10.84	0.69	10.292
3p	13.8	10.84	0.69	10.292
H $1s^a$	13.6	6.44	−12.9	12.848
H $1s^b$	13.6	0	0	12.848
Cu 4s	7.72	8.84	0.942	10.9
4p	3.98	6.64	1.05	10.9
3d	10.66	5.63	4.08	10.9

[a] When $-0.5 \leq q_H \leq 0.5$. [b] When $0.5 < q_H \leq 1.0$.

Acknowledgment. Our work was generously supported by the Advanced Research Projects Agency through the Materials Science Center at Cornell University and by the National Science Foundation. We are grateful to a knowledgeable referee for his comments and for providing us with useful additional references.

Appendix 1

Consider two interacting Ni(II) ions with high spin ($S_A = 1$) ground states $(t_{2g})^6(e_g)^2$. In the dimer there will be four e_g-like MO's: ϕ_1, ϕ_2, ϕ_3, ϕ_4. From these four e_g orbitals one forms orthogonalized localized orbitals on each center A and B

$$\frac{1}{\sqrt{2}}(\phi_1 + \phi_2) = \phi_a \sim z_A^2$$

$$\frac{1}{\sqrt{2}}(\phi_1 - \phi_2) = \phi_2 \sim z_B^2$$

$$\frac{1}{\sqrt{2}}(\phi_3 + \phi_4) = \phi_b \sim (x^2 - y^2)_A$$

$$\frac{1}{\sqrt{2}}(\phi_3 - \phi_4) = \phi_2 \sim (x^2 - y^2)_B$$

The wave functions for the $S = 2$, 1, and 0 states of the dimer are

$$\psi_2^0 = |abcd\chi_2| \quad \chi_2 = \alpha\alpha\alpha\alpha$$

$$\psi_1^0 = |abcd\chi_1| \quad \chi_1 = (\alpha\beta + \beta\alpha)\alpha\alpha - \alpha\alpha(\alpha\beta + \beta\alpha)$$

$$\psi_0^0 = |abcd\chi_0| \quad \chi_0 = (\alpha\beta + \beta\alpha)(\alpha\beta + \beta\alpha) - 2\alpha\alpha\beta\beta - 2\beta\beta\alpha\alpha$$

The compact notation for the Slater determinants differs somewhat from that used previously but is self-evident. The corresponding energies are

$$E_2^0 = E^0 - K$$

$$E_1^0 = E^0$$

$$E_0^0 = E^0 + \tfrac{1}{2}K$$

$$K = K_{ac} + K_{ad} + K_{bc} + K_{bd} > 0$$

$$E^0 = h_a + h_b + h_c + h_d + \sum_{\substack{i,j \\ i>j}}^{4} J_{ij} - K_{cd} - K_{ab}$$

The possible "ionic" configurations are

$$\psi_1^a(a \rightarrow c) = |ccbd(\alpha\beta\alpha\alpha)|$$
$$\psi_1^b(b \rightarrow d) = |ddac(\alpha\beta\alpha\alpha)|$$
$$\psi_1^c(c \rightarrow a) = |aabd(\alpha\beta\alpha\alpha)|$$
$$\psi_1^d(d \rightarrow b) = |bbac(\alpha\beta\alpha\alpha)|$$

for $S = 1$ and analogous ones for $S = 0$. None are possible for $S = 2$.

After configuration mixing the new energies are

$$E_2 = E_2^0$$
$$E_1 = E_1^0 - \frac{2V_{ac}^2}{E_1(a \rightarrow c) - E_1^0} - \frac{2V_{bd}^2}{E(b \rightarrow d) - E_1^0}$$
$$E_0 = E_0^0 - \frac{3V_{ac}^2}{E_0(a \rightarrow c) - E_0^0} - \frac{3V_{bd}^2}{E_0(b \rightarrow d) - E_0^0}$$
$$E_1(a \rightarrow c) - E_1^0 = E_0(a \rightarrow c) - E_0^0 = J_{aa} - J_{ac}$$
$$E_1(b \rightarrow d) - E_1^0 - E_0(b \rightarrow d) - E_0^0 = J_{bb} - J_{bd}$$
$$V_{ac} = \langle c|h + J_a + J_b + J_d - K_d|a\rangle$$
$$V_{bd} = \langle d|h + J_a + J_b + J_c - K_c|b\rangle$$

where only coulomb two-electron integrals have been kept in $E_1(a \rightarrow c)$ and $E_1(b \rightarrow d)$.

The Hartree-Fock Hamiltonian of the high-spin state can be written

$$H_{HF} = h + J_a - K_a + J_b - K_b + J_c - K_c + J_d - K_d$$
$$= h + J_1 - K_1 + J_2 - K_2 + J_3 - K_3 + J_4 - K_4$$
$$\phi_1 = (a + c)/\sqrt{2} \qquad \phi_3 = (b + d)/\sqrt{2}$$
$$\phi_2 = (a - c)/\sqrt{2} \qquad \phi_4 = (b - d)/\sqrt{2}$$
$$\epsilon_1 - \epsilon_2 = 2\langle a|h + J_b - K_b + J_d - K_d|c\rangle$$
$$\epsilon_1 - \epsilon_2 = 2V_{ac} + \langle aa|ac\rangle + \text{smaller terms}$$
$$\epsilon_3 - \epsilon_4 = 2V_{bd} + \langle bb|bd\rangle + \text{smaller terms}$$
$$E_2 - E_1 = -4J = V - K$$
$$E_1 - E_0 = -2J = \tfrac{1}{2}V - \tfrac{1}{2}K$$
$$K = K_{ac} + K_{ad} + K_{bc} + K_{bd}$$
$$V \cong \frac{\frac{1}{2}(\epsilon_1 - \epsilon_2)^2}{J_{aa} - J_{ac}} + \frac{\frac{1}{2}(\epsilon_3 - \epsilon_4)^2}{J_{bb} - J_{bd}}$$

Thus the J of the spin Hamiltonian can be decomposed into a ferromagnetic term (K) and an antiferromagnetic term (V) which depends on the splittings of the pairs of MO's.

Appendix 2

Computational Procedures. Calculations were carried out using the extended Hückel (EH) method with off-diagonal matrix elements given by the expression

$$H_{ij} = 1.75S_{ij}(H_{ii} + H_{jj})/2$$

The atomic orbital energies H_{ii} were obtained from self-consistent charge (SCC) EH calculations.[81] In these iterative calculations the H_{ii}'s depend on the total charge on the atom, q_A, and on the charge, q_j, associated with orbitals on other atoms through the expression

$$H_{ii} = -C_i - 0.9(B_i q_A + A_i q_A^2) - \sum_{B \neq A} \sum_{j \in B} q_j \gamma_{ij}$$

where γ_{ij}, the two-center electron repulsion parameter, is given by the Ohno[82] expression

Table V. Atomic H_{ii} Parameters for Cu Dimer Compounds (eV): A = $[Cu_2Cl_6]^{2-}$, B = $[Cu_2(OH)_2Cl_4]^{2-}$, C = $[Cu_2(OCH_3)_2Cl_4]^{2-}$, D = $Cu_2(HCOO)_4$, E = $Cu_2(pyO)_2Cl_4$, F = $[Cu_2(C_2O_4)Cl_8]^{6-}$

	A	B	C	D	E	F
Cu 4s	−11.44	−9.57	−9.32	−11.23	−9.58	−9.57
4p	−6.06	−3.32	−3.35	−5.56	−3.32	−3.22
3d	−14.00	−13.84	−12.86	−14.19	−13.84	−13.34
O 2s		−32.16	−29.84	−33.17	−31.02	−30.66
2p		−15.63	−13.31	−16.64	−14.49	−14.13
Cl 3s	−27.08	−26.46	−25.31		−26.46	−26.46
3p	−15.58	−14.96	−13.81		−14.96	−14.96
C 2s			−22.55	−24.52	−24.02[a]	−22.57
2p			−13.71	−15.69	−15.18[a]	−13.73
H 1s		−5.12	−17.32	−17.91	−17.05[a]	
N 2s					−29.44	
2p					−17.08	

[a] Not all atoms equivalent.

$$\gamma_{ij} = [R_{AB}^2 + [\tfrac{1}{2}(\gamma_{ii} + \gamma_{jj})]^{-2}]^{-1/2}$$

The parameters C_i, B_i, A_i, and γ_{ii} are given in Table IV.

The γ_{ii} one-center electron repulsion parameters were taken from Whitehead[83] for main group elements, and the parameters A, B, and C were determined from experimental ionization potentials and electron affinities. The parameters A, B, and C for Cu are based on valence-state ionization potentials from Ballhausen and Gray.[84]

The charge q_i associated with orbital i is defined as

$$q_i = P_i^0 - P_i$$
$$q_A = q_s + q_p + q_d$$

where P_i is the orbital population computed by a Mulliken analysis and P_i^0 is the orbital population of the neutral atom. For charged molecules a Madelung energy correction is applied to H_{ii} so that the corrected H_{ii}'s may be used in a normal EH calculation.

$$H_{ii} = H_{ii} - \Delta G_{av}$$
$$\Delta G_{ii} = -\frac{q}{N} \sum_k P_k \gamma_{ik}$$

where ΔG_{av} is ΔG_{ii} averaged over all orbitals and N is the number of electrons. Finally a modified form of H_{ij} is used in the SCC process for charged species.

$$H_{ij} = 1.75S_{ij}(H_{ii} + H_{jj})/2 + 0.75S_{ij}(\Delta G_{ii} + \Delta G_{jj})/2$$

Orbital exponents were chosen using Slater's rules for C (1.625), N (1.95), and O (2.275); other exponents used were H (1.3) and Cl (2.03).[85] In some instances the exponent for the O 2s orbital and the Cl 3s orbital was raised to 2.7 to reduce interactions with these low-lying orbitals. The 4s and 4p exponents (1.55) for Cu were taken from Richardson,[86] as well as the two-component 3d orbital of Cu^+ with exponents of 5.95 and 2.30 and relative weights of 0.59332 and 0.57442, respectively.

Since charge iterative calculations on the metal dimers themselves were deemed not practical for our purposes, the H_{ii}'s were determined from a SCC calculation on an appropriate monomer species. In one instance, $[Cu_2Cl_6^{2-}]$, a calculation was carried out on the dimer, and the resulting values were in good agreement with the $CuCl_4^{2-}$ values.

For the acetate, pyridine N-oxide, and oxalate series where no truly representative monomer exists, the SCC calculations were performed on the ligands themselves, usually with a point charge at the metal sites (see below). The resulting H_{ii}'s were all raised by a constant value for the dimer calculation. A representative set of H_{ii} values appears in Table V.

For example, in the acetate series of calculations the H_{ii}'s of Cu and O were obtained from a SCC calculation on

square planar $[Cl_3Cu(OCHO)]^{2-}$. Separate calculations were performed on the $XCOO^-$ ligand with two point charges ($q = +0.5$) at the metal positions. Previous calculations on the OCH_2X^- series had shown this to be a reasonable assumption. The H_{ii} atomic levels of $HCOO^-$ were shifted to match the results from the Cu complex, and the levels of the other $XCOO^-$ ligands were adjusted accordingly for the dimer. Finally the actual dimer considered was $Cu_2(HCOO)_2(XCOO)_2$ where substituents were placed only on two opposite carbon atoms.

For the pyridine *N*-oxide series, SCC calculations on the ligand in the presence of a point charge ($q = +1.0$) 2.0 Å from the O were used to determine the ligand levels. These were arbitrarily lowered 5 eV for the dimer calculation; Cu and Cl values were taken from the $Cu(OH)_2Cl_2$ calculation.

The same technique was used for the oxalate dimer, with two point charges ($q = +1.0$) located at the metal position. A constant shift of −3.5 eV was then added. When SCC calculations of this type were attempted on Cu complexes of ligands with extended π systems, the results usually showed the lowest virtual π^* level to lie below the highest occupied d level. This perhaps arises from our choice of a single constant in the formula for H_{ij}, while some investigators have advocated different constants for σ and π orbitals.[87]

References and Notes

(1) R. L. Martin in "New Pathways in Inorganic Chemistry", E. A. V. Ebsworth, A. G. Maddock, and A. G. Sharpe, Ed., Cambridge University Press, London, 1968, Chapter 9.
(2) P. W. Ball, *Coord. Chem. Rev.*, **4**, 361 (1969); G. E. Kokoszka and R. W. Duerst, *ibid.*, **5**, 209 (1970); E. Sinn, *ibid.*, **5**, 313 (1970).
(3) M. Kato, H. B. Jonassen, and J. C. Fanning, *Chem. Rev.*, **64**, 99 (1964).
(4) A. P. Ginsberg, *Inorg. Chim. Acta Rev.*, **5**, 45 (1971).
(5) H. B. Gray, *Adv. Chem. Ser.*, **No. 100**, 365 (1971).
(6) (a) P. A. M. Dirac, *Proc. R. Soc. London, Ser. A*, **112**, 661 (1926); **123**, 714 (1929); (b) W. Heisenberg, *Z. Phys.*, **38**, 411 (1926); **49**, 619 (1928); (c) J. H. Van Vleck, "Theory of Electric and Magnetic Susceptibilities", Oxford University Press, London, 1932.
(7) P. W. Anderson, *Solid State Phys.*, **14**, 99 (1963).
(8) (a) J. B. Goodenough, "Magnetism and the Chemical Bond", Interscience, New York, N.Y., 1963; *Phys. Rev.*, **100**, 504 (1955); *Phys. Chem. Solids*, **6**, 287 (1958); (b) J. Kanamori, *ibid.*, **10**, 87 (1959).
(9) N. L. Huang and R. Orbach, *Phys. Rev.*, **154**, 487 (1967); N. L. Huang, *ibid.*, **157**, 378 (1967); D. E. Rimmer, *J. Phys. C*, **2**, 329 (1969); C. G. Barraclough and R. W. Brookes, *J. Chem. Soc., Faraday Trans.*, 1364 (1974).
(10) A. E. Hansen and C. J. Ballhausen, *Trans. Faraday Soc.*, **61**, 631 (1955).
(11) I. G. Dance, *Inorg. Chim. Acta*, **9**, 77 (1974); *Inorg. Chem.*, **12**, 2743 (1973).
(12) R. Hoffmann, *Acc. Chem. Res.*, **4**, 1 (1971); R. Gleiter, *Angew. Chem.*, **86**, 770 (1974).
(13) C. K. Jørgensen, "Absorption Spectra and Chemical Bonding in Complexes", Pergamon Press, Oxford, 1962, p 207; "Modern Aspects of Ligand Field Theory", North Holland Publishing Co., Amsterdam, 1971, p 317, 318.
(14) R. W. Jotham and S. F. A. Kettle, *Inorg. Chem.*, **9**, 1390 (1970).
(15) (a) L. Salem and C. Rowland, *Angew. Chem.*, **84**, 86 (1972); *Angew. Chem., Int. Ed. Engl.*, **11**, 92 (1972); (b) J. F. Harrison in "Carbene Chemistry", 2nd ed, W. Kirmse, Ed., Academic Press, New York, N.Y., 1971.
(16) W. A. Goddard, III, *J. Chem. Phys.*, **48**, 450 (1968); W. A. Goddard, III, T. H. Dunning, Jr., W. J. Hunt, and P. J. Hay, *Acc. Chem. Res.*, **6**, 368 (1973); P. J. Hay, Dissertation, California Institute of Technology, 1972.
(17) P.-O. Lowdin, *Phys. Rev.*, **97**, 1474 (1955).
(18) R. Hoffmann, *J. Chem. Phys.*, **39**, 1397 (1963); R. Hoffmann and W. N. Lipscomb, *ibid.*, **36**, 2179, 3489 (1962); **37**, 2782 (1962).
(19) D. J. Hodgson, *Prog. Inorg. Chem.*, **19**, 173 (1975); Abstracts, 167th National Meeting of the American Chemical Society, Los Angeles, Calif., April 1974, INOR 139; "Extended Interactions between Metal Ions in Transition Metal Complexes", L. V. Interrante, Ed., ACS Symposium Series No. 5, American Chemical Society, Washington, D.C., 1974, p 94.
(20) L. L. Lohr and W. N. Lipscomb, *Inorg. Chem.*, **2**, 911 (1963).
(21) (a) M. Yevitz and J. A. Stanko, *J. Am. Chem. Soc.*, **93**, 1512 (1971); (b) E. Pederson, *Acta Chem. Scand.*, **26**, 333 (1972); (c) A. Urushiyama, T. Nomura, and M. Nakahara, *Bull. Chem. Soc. Jpn.*, **43**, 3971 (1970); (d) J. T. Veal, D. Y. Jeter, J. C. Hempel, R. P. Eckberg, W. E. Hatfield, and D. J. Hodgson, *Inorg. Chem.*, **12**, 2928 (1973); (e) S. J. Lippard, H. Schugar, and C. Walling, *ibid.*, **6**, 1825 (1967).
(22) J. D. Dunitz and L. E. Orgel, *J. Chem. Soc.*, 2594 (1953).
(23) B. Jezowska-Trzebiatowska and W. Wojciechowski, *Zh. Strukt. Khim.*, **4**, 872 (1963); B. Jezowska-Trzebiatowska, H. Kozlowski, and L. Natkaniec, *Bull. Acad. Pol. Sci., Ser. Chim.*, **19**, 115 (1971); B. Jezowska-Trzebiatowska, *Pure Appl. Chem.*, **27**, 89 (1971); B. Jezowska-Trzebiatowska, H. Kozlowski, T. Cukierda, and A. Ozarowski, *J. Mol. Struct.*, **19**, 663 (1973); B. Jezowska-Trzebiatowska and W. Wojciechowski *Transition Met. Chem.*, **6**, 1 (1970).
(24) J. Glerup, *Acta Chem. Scand.*, **26**, 3775 (1972). See also E. Larsen and G. N. La Mar, *J. Chem. Educ.*, **51**, 633 (1974).
(25) H. J. Schugar, G. R. Rossmann, and H. B. Gray, *J. Am. Chem. Soc.*, 91, 4564 (1969).
(26) D. Baumann, H. Endres, H. J. Keller, and J. Weiss, *J. Chem. Soc., Chem. Commun.*, 853 (1973).
(27) (a) K. T. McGregor, N. T. Watkins, D. L. Lewis, R. F. Drake, D. J. Hodgson, and W. E. Hatfield, *Inorg. Nucl. Chem. Lett.*, **9**, 423 (1973), and references therein; (b) D. L. Lewis, W. E. Hatfield, and D. J. Hodgson, *Inorg. Chem.*, **11**, 2216 (1972); (c) D. L. Lewis, K. T. McGregor, W. E. Hatfield, and D. J. Hodgson, *ibid.*, **13**, 1013 (1974); (d) E. D. Estes, W. E. Hatfield, and D. J. Hodgson, *ibid.*, **13**, 1654 (1974).
(28) J. A. Bertrand and C. E. Kirkwood, *Inorg. Chim. Acta*, **6**, 248 (1972); J. A. Bertrand, J. H. Smith, and P. G. Eller, *Inorg. Chem.*, **13**, 1649 (1974).
(29) (a) R. D. Willett, *J. Chem. Soc., Chem. Commun.*, 607 (1973); (b) R. D. Willett and C. Chow, *Acta Crystallogr., Sect. B*, **30**,207 (1974); (c) C. Chow, R. Caputo, R. D. Willett, and B. C. Gerstein, *J. Chem. Phys.*, **61**, 271 (1974).
(30) (a) S. C. Abrahams and H. J. Williams, *J. Chem. Phys.*, **39**, 2923 (1963); (b) P. H. Vossos, D. R. Fitzwater, and R. E. Rundle, *Acta Crystallogr.*, **16**, 1045 (1963).
(31) (a) R. D. Willett, C. Dwiggins, Jr., R. T. Kruh, and R. E. Rundle, *J. Chem. Phys.*, **38**, 2429 (1963); (b) G. J. Maass, B. C. Gerstein, and R. D. Willett, *ibid.*, **46**, 401 (1967).
(32) (a) R. D. Willett, *J. Chem. Phys.*, **44**, 39 (1966); (b) B. C. Gerstein, F. D. Gehring, and R. D. Willett, *J. Appl. Phys.*, **43**, 1932 (1972).
(33) M. Textor, E. Dubler, and H. R. Oswald, *Inorg. Chem.*, **13**, 1361 (1974).
(34) In these calculations we again adopted an increased orbital exponent of 2.7 for the Cl 3s, since the 3d (Cu)–3s (Cl) interactions otherwise apparently are overestimated by the extended Hückel method.
(35) R. D. Willett and O. L. Liles, Jr., *Inorg. Chem.*, **6**, 1666 (1967).
(36) R. Mason and D. M. P. Mingos, *J. Organomet. Chem.*, **50**, 53 (1973).
(37) B. K. Teo, M. B. Hall, R. F. Fenske, and L. F. Dahl, *J. Organomet. Chem.*, **70**, 413 (1974).
(38) D. M. Duggan, R. G. Jungst, K. R. Mann, G. D. Stucky, and D. N. Hendrickson, *J. Am. Chem. Soc.*, **96**, 3443 (1974).
(39) J. A. Carrabine and M. Sundaralingam, *J. Am. Chem. Soc.*, **92**, 369 (1970); M. Sundaralingam and J. A. Carrabine, *J. Mol. Biol.*, **61**, 287 (1971); J. P. Declercq, M. Debbaudt, and M. Van Meerssche, *Bull. Soc. Chim. Belg.*, **80**, 527 (1971).
(40) (a) D. J. Hodgson, P. K. Hale, and W. E. Hatfield, *Inorg. Chem.*, **10**, 1061 (1971); (b) E. D. Estes, W. E. Estes, W. E. Hatfield, and D. J. Hodgson, *ibid.*, **14**, 106 (1975), and references therein.
(41) D. H. Svedung, *Acta Chem. Scand.*, **23**, 2865 (1969).
(42) V. F. Duckworth and N. C. Stephenson, *Acta Crystallogr., Sect. B*, **25**, 1795 (1969).
(43) (a) J. F. Villa, *Inorg. Chem.*, **12**, 2054 (1973); (b) R. F. Drake, V. H. Crawford, N. W. Laney, and W. E. Hatfield, *ibid.*, **13**, 1246 (1974).
(44) For a general account of transition metal pentacoordination see A. R. Rossi and R. Hoffmann, *Inorg. Chem.*, **14**, 365 (1975).
(45) D. Y. Jeter, D. L. Lewis, J. C. Hempel, D. J. Hodgson, and W. E. Hatfield, *Inorg. Chem.*, **11**, 1958 (1972); see also ref 19.
(46) B. Bleaney and K. D. Bowers, *Proc. R. Soc. London, Ser. A*, **214**, 451 (1952).
(47) J. N. van Niekerk and F. K. L. Schoening, *Acta Crystallogr.*, **6**, 227 (1953).
(48) (a) R. W. Jotham, S. F. A. Kettle, and J. A. Marks, *J. Chem. Soc., Dalton Trans.*, 428 (1972), and references therein; (b) J. A. Moreland and R. J. Doedens, *J. Am. Chem. Soc.*, **97**, 508 (1975). The dimensions of the trifluoroacetate dimer differ significantly from those of the acetate.
(49) (a) B. N. Figgis and R. L. Martin, *J. Chem. Soc.*, 3837 (1956); (b) I. G. Ross, *Trans. Faraday Soc.*, **55**, 1057 (1959); I. G. Ross and J. Yates, *ibid.*, **55**, 1064 (1959); (c) L. S. Forster and C. J. Ballhausen, *Acta Chem. Scand.*, **16**, 1385 (1962); (d) E. A. Boudreaux, *Inorg. Chem.*, **3**, 506 (1964); (e) M. Kato, H. B. Jonassen, and J. C. Fanning (with a contribution by L. C. Cusachs), *Chem. Rev.*, **64**, 99 (1964); (f) D. J. Royer, *Inorg. Chem.*, **4**, 1830 (1965); (g) L. Dubicki and R. L. Martin, *ibid.*, **5**, 2203 (1966); (h) A. Bose, R. N. Bagchi, and P. Sen Gupta, *Indian J. Phys.*, **42**, 55 (1968); (i) I. B. Bersuker and Yu. G. Titova, *Teor. Eksp. Khim.*, **6**, 469 (1970); (j) A. K. Gregson, R. L. Martin and S. Mitra, *Proc. R. Soc. London*, 320, 473 (1971).
(50) (a) M. L. Tonnet, S. Yamada, and I. G. Ross, *Trans. Faraday Soc.*, **60**, 840 (1964); (b) G. F. Kokoszka, H. C. Allen, Jr., and G. Gordon, *J. Chem. Phys.*, **42**, 3693 (1965).
(51) A previous semiempirical MO calculation exists: L. C. Cusachs, G. L. Cusachs, B. L. Trus, and J. R. Linn, Jr., cited in Y. Muto, M. Kato, H. B. Jonassen, and L. C. Cusachs, *Bull. Chem. Soc. Jpn.*, **42**, 417 (1969). An S–A splitting of 0.3 eV is reported.
(52) D. M. L. Goodgame, N. J. Hill, D. F. Marsham, A. C. Skapski, M. L. Smart, and P. G. H. Troughton, *Chem. Commun.*, 629 (1969).
(53) (a) B. Morosin, R. C. Hughes, and Z. G. Soos, *Acta Crystallogr., Sect. B*, **31**, 762 (1975); (b) J. S. Valentine, A. J. Silverstein, and Z. G. Soos, *J. Am. Chem. Soc.*, **96**, 97 (1974).
(54) G. M. Brown and R. Chidambaram, *Acta Crystallogr., Sect. B*, **29**, 2393 (1973).
(55) (a) M. Corbett and B. F. Hoskins, *Chem. Commun.*, 1602 (1968); (b) M. F. Rudolf, B. Jasiewicz, and B. Jezowska-Trzebiatowska, *Bull. Acad. Pol. Sci., Ser. Sci. Chim.*, **22**, 351 (1974).
(56) (a) M = Cr: L. R. Ocone and B. P. Block, *Inorg. Synth.*, **8**, 125 (1966); J. N. van Niekerk, F. R. L. Schoening, and J. F. DeWet, *Acta Crystallogr.*, **6**, 501 (1953), report the structure of the dihydrate. (b) M = Mo: T. A. Stephenson, E. Bannister, and G. Wilkinson, *J. Chem. Soc.*, 2538 (1964); D. Lawton and R. Mason, *J. Am. Chem. Soc.*, **87**, 921 (1965); F.

A. Cotton and J. G. Norman, Jr., *J. Coord. Chem.*, **1**, 161 (1971). (c) M_2 = CrMo: C. D. Garner and R. G. Senior, *J. Chem. Soc., Chem. Commun.*, 580 (1974).
(57) R. W. Jotham, S. F. A. Kettle, and J. A. Marks, *J. Chem. Soc., Dalton Trans*, 1133 (1972).
(58) Y. Muto, M. Kato, H. B. Jonassen, and L. C. Cusachs, *Bull. Soc. Chim. Jpn.*, **42**, 417 (1969).
(59) M. R. Kidd and W. H. Watson, *Inorg. Chem.*, **8**, 1886 (1969).
(60) (a) H. L. Schäfer, J. C. Morrow, and H. M. Smith, *J. Chem. Phys.*, **42**, 504 (1965); (b) R. S. Sager, R. J. Williams, and W. H. Watson, *Inorg. Chem.*, **6**, 951 (1967); **8**, 694 (1969); (c) W. H. Watson and D. R. Johnson, *J. Coord. Chem.*, **1**, 145 (1971).
(61) N. F. Curtis, I. R. N. McCormick, and T. N. Waters, *J. Chem. Soc., Dalton Trans.*, 1537 (1973).
(62) D. M. Duggan, E. K. Barefield, and D. N. Hendrickson, *Inorg. Chem.*, **12**, 985 (1973).
(63) D. M. Duggan and D. H. Hendrickson, *Inorg. Chem.*, **12**, 2422 (1973).
(64) In the model dimer which we calculated, we replaced the terminal N-containing ligands by chlorines. The other structural parameters used were *R*(Cu–Cl) = 2.26 Å, *R*(Cu–O) = 2.10 Å, Cl–Cu–Cl angle = 90°, and O–C–C angle = 125°.
(65) R. Hoffmann and R. B. Davidson, *J. Am. Chem. Soc.*, **93**, 5699 (1971).
(66) T. N. Polynova, T. V. Filippova, M. A. Porai-Koshits, and L. I. Marmynenko, *Zh. Strukt. Khim.*, **11**, 558 (1973).
(67) A crystal structure of the $O_3MoEDTAMoO_3^{4-}$ ion shows the two octahedrally coordinated Mo(VI) centers bridged by a fully extended EDTA chain: J. J. Park, M. D. Glick, and J. L. Hoard, *J. Am. Chem. Soc.*, **91**, 301 (1969). Mo(V), d^1, complexes with two Mo centers and a single EDTA type ligand have been synthesized: R. L. Pecsok and D. T. Sawyer, *J. Am. Chem. Soc.*, **78**, 5496 (1956); L. V. Haines and D. T. Sawyer, *Inorg. Chem.*, **6**, 2147 (1967). Crystal structures of two compounds in this series reveal a dioxo-bridged structure: R. M. Wing and K. P. Callahan, *Inorg. Chem.*, **8**, 2303 (1969).
(68) D. M. P. Mingos and I. Ghatak, Queen Mary College, private communication.
(69) (a) E. D. Stevens and J. T. Yoke, *Inorg. Chim. Acta*, **4**, 244 (1970); (b) G. J. Tennenhouse, Ph.D. Dissertation, University of Illinois, 1963; (c) H. M. Hilliard, D. D. Axtell, M. M. Gilbert, and J. T. Yoke, *J. Inorg. Nucl. Chem.*, **31**, 2117 (1969).
(70) J. F. Villa and W. E. Hatfield, *J. Am. Chem. Soc.*, **93**, 4081 (1971).
(71) A. Santoro, A. D. Mighell, and C. W. Reimann, *Acta Crystallogr., Sect. B*, **26**, 979 (1970).
(72) G. F. Kokoszka and C. W. Reimann, *J. Inorg. Nucl. Chem.*, **32**, 3229 (1970).
(73) D. E. Billing, A. E. Underhill, D. M. Adams, and D. M. Morris, *J. Chem. Soc. A*, 902 (1966).
(74) K. Hyde, G. F. Kokoszka, and G. Gordon, *J. Inorg. Nucl. Chem.*, **31**, 1993 (1969).
(75) M. J. M. Campbell, R. Grzeskowiak, and F. B. Taylor, *J. Chem. Soc. A*, 19 (1970).
(76) G. W. Inman, Jr., J. A. Barnes, and W. E. Hatfield, *Inorg. Chem.*, **11**, 764 (1972); G. W. Inman, Jr., and W. E. Hatfield, *ibid.*, **11**, 3085 (1972); H. W. Richardson, W. E. Hatfield, H. J. Stoklosa, and J. R. Wasson, *ibid.*, **12**, 2051 (1973).
(77) R. W. Matthews and R. A. Walton, *Inorg. Chem.*, **10**, 1433 (1971).
(78) E. B. Fleischer and M. B. Lawson, *Inorg. Chem.*, **11**, 2772 (1972).
(79) P. W. Carreck, M. Goldstein, E. M. McPartlin, and W. D. Unsworth, *Chem. Commun.*, 1634 (1971); M. Goldstein, F. B. Taylor, and W. D. Unsworth, *J. Chem. Soc., Dalton Trans.*, 418 (1972).
(80) (a) C. Creutz and H. Taube, *J. Am. Chem. Soc.*, **91**, 3988 (1969); **95**, 1086 (1973); R. H. Magnuson and H. Taube, *ibid.*, **94**, 7213 (1972); S. S. Isied and H. Taube, *ibid.*, **95**, 8198 (1973). (b) See also B. Mayoh and P. Day, *J. Am. Chem. Soc.*, **94**, 2885 (1972); E. B. Fleischer and D. K. Lavallee, *ibid.*, **94**, 2599 (1972); J. H. Elias and R. S. Drago, *Inorg. Chem.*, **11**, 415 (1972); S. A. Adeyemi, E. C. Johnson, F. J. Miller, and T. L. Meyer, *ibid.*, **12**, 2371 (1973), and references therein.
(81) The charge iterative calculations described here differ from many traditional approaches by the inclusion of two-center Coulomb terms (see text). A more complete discussion will be published separately by J. C. Thibeault.
(82) K. Ohno, *Theor. Chim. Acta*, **2**, 219 (1964); G. Klopman, *J. Am. Chem. Soc.*, **86**, 1463 (1964).
(83) M. A. Whitehead in "Sigma Molecular Orbital Theory", O. Sinanoglu and K. Wiberg, Ed., Yale, 1970, p 50.
(84) C. J. Ballhausen and H. B. Gray, "Molecular Orbital Theory", W. A. Benjamin, New York, N.Y., 1964.
(85) E. Clementi and D. L. Raimondi, *J. Chem. Phys.*, **38**, 2686 (1963).
(86) J. W. Richardson, W. C. Nieuwpoort, R. R. Powell, and W. F. Edgell, *J. Chem. Phys.*, **36**, 1057 (1962).
(87) L. C. Cusachs, *J. Chem. Phys.*, **43**, S157 (1965).

An X-Ray Photoelectron Spectroscopic Study of Charge Distributions in Tetracovalent Compounds of Nitrogen and Phosphorus

Winfield B. Perry, Theodore F. Schaaf, and William L. Jolly*

Contribution from the Department of Chemistry, University of California and the Inorganic Materials Research Division of the Lawrence Berkeley Laboratory, Berkeley, California 94720. *Received November 25, 1974*

Abstract: Core electron binding energies for ten phosphorus and four nitrogen compounds have been measured by X-ray photoelectron spectroscopy in the gas phase. The chemical shifts have been correlated by the electrostatic potential equation using charge distributions from extended Hückel theory and CNDO/2 molecular orbital calculations. The data indicate that resonance structures of the type R_3M^+-X^- (I) contribute significantly to the charge distributions in the tetracovalent compounds. The data for the phosphorus compounds can be fairly well rationalized without the inclusion of any $p\pi \rightarrow d\pi$ bonding between the central atom and the X ligand, but the effects of electronic relaxation upon the core binding energy chemical shifts must be included.

The bonding in four-coordinate compounds of nitrogen and phosphorus can be represented by I. However, because

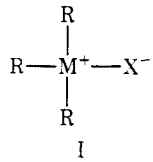

I

these compounds generally have short M–X bond lengths and high M–X stretching frequencies, multiple bond character has been postulated for the M–X bonds. Such multiple bonding can be explained by hyperconjugation, i.e., no-bond resonance,[1,2] II. When the central atom is phosphorus, however, it is conceivable that the phosphorus 3d orbitals

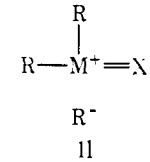

II

may significantly participate in the bonding.[2-4] In this case, a resonance structure having no formal charges, such as III, would be appropriate. The latter structure implies $p\pi \rightarrow d\pi$ bonding between the central phosphorus atom and the peripheral X ligand.